AR-008-937

DSTO-TR-0068

Laser Ignition of Explosives, Pyrotechnics and Propellants: A Review

Leo de Yong, Tam Nguyen and John Waschl

DEPARTMENT OF DEFENCE

DEFENCE SCIENCE AND TECHNOLOGY ORGANISATION

Laser Ignition of Explosives, Pyrotechnics and Propellants: A Review

Leo de Yong, Tam Nguyen and John Waschl

Weapons Systems Division
Aeronautical and Maritime Research Laboratory

DSTO-TR-0068

ABSTRACT

This review critically examines the current state of technology of laser ignition of explosives, pyrotechnics and propellants. It presents the approaches used for each energetic material, looks at the materials tested, the results obtained and the potential for future development of in-service laser initiated ordnance.

It has been concluded that the only possible approach to laser initiation of explosives in a fuze is via a laser driven flyer plate but that the current cost and size of prototypes are too great for incorporation in most practical systems.

Laser ignition of pyrotechnics in terms of pyrotechnic materials and igniter design has reached a significant degree of maturity and it is only a matter of time before laser actuated pyrotechnic igniters are qualified for in-service use.

For propellants, the principle application of laser ignition technology is in the assessment of the overall hazard potential of the material with respect to planned and accidental stimuli, and in the verification of ignition theories and the determination of global energetic and kinetic parameters. In general solid propellants are initiated by pyrotechnic igniters and the practical development of a direct laser initiation system for rocket or gun propellants is not considered a possibility in the short term.

DEPARTMENT OF DEFENCE

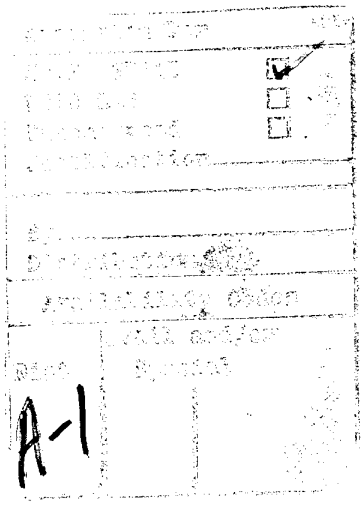

Published by

DSTO Aeronautical and Maritime Research Laboratory
PO Box 4331
Melbourne Victoria 3001

Telephone: (03) 9626 8111
Fax: (03) 9626 8999

AR No. 008-937
May 1995

APPROVED FOR PUBLIC RELEASE

Laser Ignition of Explosives, Pyrotechnics and Propellants: A Review

EXECUTIVE SUMMARY

This review critically examines the current state of technology of laser initiation of explosives, pyrotechnics and propellants. It presents the approaches used for each energetic material, looks at the materials tested, the results obtained and the potential for future development of in-service laser initiated ordnance.

Laser initiation has many advantages when compared to conventional bridgewire initiation. The principle ones are their immunity from stray electromagnetic fields, electrostatic discharge or stray electrical energy, the potential for use of less sensitive explosives or pyrotechnics in the initiator due to the greater power output of the laser, and the greater versatility with wholly electronic safety and arming, built in self test, and multipoint simultaneous initiation.

Laser initiation of high explosives (HE's) by optical means began in the early 1960's. The wavelengths used ranged from 0.266 μm to 1.06 μm and Ruby, CO_2, eximer and Nd-YAG lasers have been employed. All the lasers operate in a pulsed mode and deliver iradiances in the GW/cm^2 range.

Laser initiation of HE's has been attempted three ways: (a) direct interaction with the HE; (b) rapid heating of a thin film in contact with a HE; and (c) ablating a thin metal foil to produce a high velocity flyer plate that impacts the HE. Each of these approaches has been discussed.

By adjusting the HE density, purity and surface area, it is possible to initiate a range of HE's (HNS, PETN, RDX and tetryl). Direct laser initiation and laser initiation via thin films in contact with the HE are unacceptable for incorporation in modern fuses, as neither technique can reliably initiate HNS (an insensitive HE used in modern fuses). The production of laser-driven flyer plates that shock initiate the HE has been shown to successfully detonate HNS promptly. Presently, the only viable approach to laser initiation of HE is therefore via laser-driven flyer plates. But the cost, size and energy requirements of suitable lasers are too great for incorporation in all but the most expensive systems. It is considered that laser initiation is not a near term practical fusing option.

Studies into laser initiation of pyrotechnics have tended to be directed in two major areas. Firstly, measurement of the sensitivity of the pyrotechnic particle to laser energy (the effects of physical and chemical characteristics of the material), and secondly, the design and testing of practical laser initiation systems. The variety of lasers used include Ruby, Nd:YAG, CO_2, Nd:Glass, argon ion, laser diodes and pyrotechnically pumped Nd: Glass rods. At the same time, the range of materials examined has been broad, encompassing typical igniter compositions, delays, smokes, flares and thermites.

Ignition of pyrotechnics is typically achieved with a laser operating in the pulsed mode (pulse length tens-hundreds of milliseconds) with irradiances in the W/cm^2 range. Significant development of prototype laser initiation systems for pyrotechnic igniters has occurred in the last few years and has reached an advanced degree of maturity. Laser ignited pyrotechnic igniters are likely to be qualified for service use in the near future.

In general solid propellants in rocket motors are initiated by pyrotechnic igniters rather than directly via laser. Although direct laser ignition is under active R&D overseas, most of the R&D is directed towards the laser as a tool for assessing and ranking propellant ignitability. This basic research can ultimately identify propellants that meet the requirements for insensitive munition developments.

The review outlines the principal ignition theories of solid propellants and compares ignition data obtained with a laser source and that with the xenon arc image furnace. The effects of changes in the propellant formulations and various types of propellants (double-base, AP composites, HMX composites, etc.) on the ease of ignitability are discussed. The practical development of a direct laser initiation system is not considered a possibility in the short term.

Authors

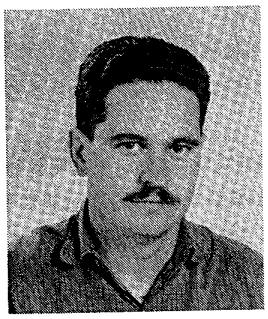

Leo de Yong
Weapons Systems Division

Leo de Yong graduated BAppSc (Chemistry) in 1977 from University of Melbourne. He worked for ICI Australia (Explosives) and Royal Melbourne Institute of Technology before joining AMRL in 1982. His work has focussed on pyrotechnics and their applications.

Tam Nguyen
Weapons Systems Division

Tam T. Nguyen holds a BSc(Hons) in Inorganic Chemistry from Sydney University and a PhD in Physical Chemistry from Newcastle University (NSW). Tam transferred from CSIRO to DSTO as a Senior Research Scientist in 1986. At present, he works in the Weapons Systems Division at Salisbury, South Australia. In the past two years, Tam managed a DSTO task on the combustion characteristics of rocket propellants. His other interests include kinetics and thermochemistry, FTIR and Raman spectroscopy of surfaces, heterogeneous catalysis and hydrocarbon conversion.

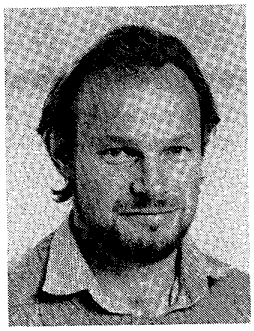

John Waschl
Weapons Systems Division

John Waschl graduated BSc (Hons) in physics from Melbourne University in 1977. He also has post graduate qualifications in Audiology and Computer Simulation. After a brief period in private industry he joined AMRL in 1982. Since then he has worked in the general field of explosives effects. During 1987-88 he was posted to Harry Diamond Laboratories (USA) where he worked on slapper detonators and electronic safety and arming systems. Currently he is engaged in slapper detonator research.

Contents

1. Introduction

Present day explosives, pyrotechnics and propellant systems are initiated by detonators, igniters, actuators or squibs and are used in many military applications including explosives ordnance, aircrew escape systems, and also in civil applications such as motor vehicle airbags. The most common method of functioning the initiator is by passing a current through a bridgewire. The energy delivered to the bridgewire heats it up, igniting the explosive or pyrotechnic material pressed onto the bridgewire, and subsequently results in the device performing the desired operation.

The one major problem with these systems is that the energetic material is not completely electrically isolated from its environment. Therefore the components are susceptible to unintended ignition by external electromagnetic radiation from radio transmitters, high power radar installations or following a nuclear event and electrostatic discharge from lightning or even a charged human operator.

Components may be protected from some of these problems to varying degrees by shielding and implementing a 1A/1W firing specification. These solutions are never one hundred percent effective and can increase the cost of the component many times. The need for the development of a safe igniter has been the primary driving force behind research into the laser ignition of pyrotechnics and high explosives.

There also exists an increasing drive towards the use of munitions incorporating fuzes that provide fast action, precise timing and versatility, but are not susceptible to hazardous stimuli. This general thrust has resulted in the development of modern fuzes that contain no moving parts and are initiated via a slapper detonator. Replacing the slapper detonator with a laser removes the electromagnetic susceptibility and provides enhanced versatility.

Unfortunatly, modern initiation techniques have not been pursued with as much vigor by the propellant community. There has been little research into the application of direct laser initiation of propellants, i.e. not involving the intermediacy of an igniter. For propellants, the principal interest has been to sudy laser initiation as a controlled ignition source for research purposes only.

This review report outlines the state of the art in laser ignition of explosives, pyrotechnics and propellants. It presents the approaches used for each energetic material and looks at the materials tested and the results obtained. It is intended that this report will be a useful reference document detailing what has been done and what the future may hold in laser ignition of energetic materials and weapons sytems.

2. Advantages of Laser Initiation Systems

Laser initiation has many advantages when compared to conventional bridgewire initiation. Some of the more obvious ones are:

(i) They are immune to accidental firings from electromagnetic fields, electrostatic discharge, or stray electrical energy;

(ii) Built in self test/checking of the integrity of the entire initiating system may be carried out without affecting the safety or the reliability of the system;

(iii) Most pyrotechnics may be initiated with low quantities of energy (mJ) and so low energy diodes may be used;

(iv) Safety and arming (S&A) systems may be made wholly electronic;

(v) Since the output energy and power of the laser can be chosen to be higher than bridgewire devices, less sensitive explosives or pyrotechnics may be used;

(vi) Since the bridgewire is eliminated, corrosion of the bridgewire is removed as a failure mechanism thus the safe/service life is lengthened and conductance of the initiator after firing is eliminated;

(vii) The laser initiator cost can be lower than corresponding 1A/1W devices;

(viii) The laser initiator can be smaller and lighter than corresponding bridgewire devices;

(ix) Laser systems may be reused several times (multiple shot capability) compared to the single shot bridgewire systems;

(x) The initiation system may be constructed in-line, removing the need for complex mechanical safety and arming systems;

(xi) Multi-point simultaneity is easily achieved; and

(xii) Distributed initiation systems are cheaper to manufacture.

3. Status of Laser Initiated Devices in Fielded Systems

The qualified in service use of laser initiated explosive, pyrotechnic or propellant ordnance has yet to be achieved.

Given the limited use of lasers with propellants, it would appear that a practical direct laser based propellant ignition system will not be seen in service for at least 10 years. In general, solid propellants in rocket motors are initiated by pyrotechnic igniters. The only system currently known to be under intense R&D activity is the Advanced Solid Rocket Motor (ASRM), a new design for the Space Shuttle Solid Rocket Booster, which contains a 48-inch diameter rocket motor incorporating a laser ignition system for the propellant. The aim of the ASRM program is to test the propellant, insulation, nozzle characteristics, laser system requirements and operation configuration [1].

There are studies underway in the US looking at the development of 20 mm Laser Initiated Caseless Ammunition (LICA). The design is based on a rapid fire gun system and the US Army is interested in expanding the concept to 155 mm guns. Research is also underway on laser ignition testing of two-piece Tank Ammunition for the Advanced Tank Canon System (ATACS). It would thus appear that the more conventional approach of using a pyrotechnic igniter to initiate the propellant is the most fruitful path for future applications.

The picture for laser based high explosive initiation systems, while more advanced than for propellants, appears to be directed toward fundamental research. Current customer interest would suggest that the production of a qualified in-line safety and arming system incorporating high explosives is likely within 8-10 years.

The development of practical laser based ignition systems using pyrotechnics is highly advanced and several active US military sponsored programs are underway. The mechanical LITES laser initiation system is being proposed for use in the egress system for the V-22 Osprey aircraft, the B-1B hybrid escape system, the F-16 egress system and the JPATS (new joint service trainer)

In relation to weapon/missile systems, possible applications that have or are being studied include the following: the Small ICBM (flew with laser ordnance), the Advanced Air to Air Missile (AAAM), the Delta Rocket System and the Advanced Rocket System.

Quantic Industries have developed several laser ordnance initiation systems based on pyrotechnic igniters. A prototype initiation system with 16 outputs has been developed for the US Ground Based Interceptor Program. In co-operation with the Korean Agency for Defence Development, Quantic has developed a laser arm-fire device (LAFD) that meets the requirements of MIL-STD-1901 "Safety Criteria for Munition Rocket and Missile Motor Ignition System Design". The application required the LAFD to be packaged in a configuration identical to that used in the Hellfire missile and testing of the first production lot in missile motors has commenced.
Quantic also markets the Model WLP200 (Nd-Glass, 150 mJ) and Model WLP100G (Nd-Glass, 500 mJ) laser initiators.

A Laser Diode Initiated Ordnance System (LDIOS) comprising a firing unit, optic energy transfer system and a pyrotechnic laser ignited squib (equivalent to the NASA Standard Initiator) has been developed for NASA. It is intended to be used to

demonstrate laser initiated ordnance for advanced satellite ordnance and release systems. It is proposed to fly these systems on the Shuttle, expendable launch vehicles and satellites by mid 1995. A flight on the Orbital Sciences Corporation Pegasus air launched space booster is planned for mid 1994. Proposed military applications of Ensign-Bickford systems are for ground launched missile and decoy systems. Ensign Bickford also has development programs with the US Navy, NASA and foreign institutions.

Universal Propulsion Company (UPCO) and Quantic Industries have developed hand portable Explosive Ordnance Disposal (EOD) systems using optical detonators for the US Navy. Both solid state laser rod and laser diode designs with portable power supplies have been produced. UPCO has also manufactured an airborne laser ordnance firing system.

Although there are many examples of practical applications for laser ordnance initiation systems, the authors are not aware of any that have been fully qualified and fielded in a practical weapon system.

The remainder of this review article provides an up to date summary of laser initiation research.

4. A Review of Research on Laser Initiation of Energetic Materials

Apart from the practical applications to weapons systems outlined above, laser ignition has also been used as a tool in the study of explosive, pyrotechnic and propellant ignition. There are significant advantages in working with a coherent, collimated beam of radiant energy. For example, the laser offers advantages in having a variable energy and power output which are independent of all other environmental parameters, it has a small beam divergence, it is easily focussed, and it has low attenuation in air. The one problem with the output of the laser is the non-homogeneous distribution of energy across the beam.

This review looks separately at laser initiation of explosives, pyrotechnics and propellants. Explosives and pyrotechnics are discussed first because of the large quantity of information available and their relative importance. Most propellants are initiated by initiating a pyrotechnic first - the primer, initiator or igniter. Consequently, the propellant section deals soley with direct propellant initiation.

The results from the many references cited in this review have often used different physical quantities to refer to the same unit (for example energy flux, energy density and energy fluence). For accuracy, clarity and uniformity the authors of this report have chosen to refer to any physical quantity with units of watts per square metre (W/m^2) or watts per square centimetre (W/cm^2) as irradiance and any physical

quantity with units of joules per square metre (J/m^2) or joules per square centimetre (J/cm^2) as radiant exposure.

4.1 Laser Ignition of Explosives

As outlined in the Introduction, the thrust for research into laser ignition of explosives is derived from the need for versatile, fast acting, and highly reliable fuzes that ideally can also meet insensitive munitions criteria.

Studies into the initiation of explosives by optical means began shortly after the advent of the laser. The wavelength employed was usually between 0.266 and 1.06 μm. Initiation was achieved with energies less than 10 J. Radiant exposure (J/cm^2) and irradiance (W/cm^2) are the common laser parameters quoted. The variety of lasers included Ruby, CO_2, excimer and Nd-YAG. All lasers were operated in a pulsed mode to deliver irradiances measured in the GW/cm^2 range.

Apart from the safety precautions required for personnel when operating these high powered lasers, a knowledge of the limitations of the laser is also important. Output radiant exposure distribution, beam divergence and pulse duration may all vary considerably depending on the output energy [2]. To overcome these problems, it is recommended that the beam intensity at the target be varied by external filters while operating the laser at a constant output. The attenuator consists of a half-wave plate and a polarising prism.

With the focused Q-switched laser pulse employed in these studies, the power handling capability of the optical components needs to be carefully specified. In addition, for irradiance above 50 GW/cm^2, it should be noted that gas breakdown at room temperature is possible and that this may affect laser target interactions [2]. For this reason high irradiance laser studies are frequently conducted at low ambient pressures.

Laser ignition of high explosives has been attempted in three ways: a) direct interaction with the HE [2-6]; b) rapid heating of a thin metal film in contact with an explosive [2,6]; and c) ablating a thin metal foil to produce a high velocity flyer plate that impacts the HE [7,8]. Each of these approaches will be discussed and evaluated in the following sections.

4.1.1 Direct Laser Initiation

In this approach the laser light interacts directly with the explosive sample. The sample is typically pressed into a receptacle that may have a window (Figure 1). If used, the window provides confinement.

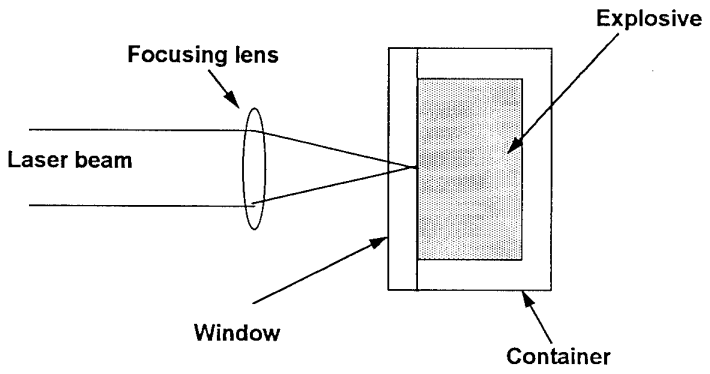

Figure 1: Schematic of the method typically employed for direct laser initiation of HE.

The sensitivity of PETN, HNS, HMX, and RDX to direct laser initiation has been reported [2-6]. Parameters of interest have included: density, particle size, specific surface area (SSA), dopant, wavelength, pulse duration, beam spot size, confinement, and confinement material.

Bykhalo et al [4] employed a Nd:YAG (1.06 μm) laser against high density (1.7 g/cm^3) PETN at a maximum of 10^5 GW/cm^2. Their one dimensional calculations indicated that the pressure at the surface would reach 500 GPa for an irradiance of 10^3 GW/cm^2. This was considered an over-estimate as in reality the interaction is not one dimensional. Nevertheless PETN was successfully initiated at ~10^3 GW/cm^2 with a spot size of about 1 mm. It was found, however, that at smaller beam spot sizes of the order of 250 μm, detonation could not be achieved at even 10^5 GW/cm^2. A critical spot size similar to the failure diameter effect was cited as the reason; the failure diameter for PETN is ≥ 300 μm [9].

The initiation energies for PETN with a Nd:YAG laser operating at 1.06 μm have been found to be lowest for PETN with a SSA of 2.1 m^2/g and density of 1.0 g/cm^3 [6]. Irradiance was of the order of 1 GW/cm^2 with beam spot size typically 0.5 mm and pulse duration 10 to 25 ns. Use of a sapphire window provided the lowest initiation energy. Others [2,5] have demonstrated a similar density effect for PETN, RDX and HMX. Tasaki et al [3] reported a similar density effect for PETN at 1.06 μm with a pulse duration of several milliseconds.

Initiation energies for PETN were found to be virtually wavelength independent for a Nd:YAG operating at 0.355, 0.532 and 1.06 μm [6]. The initiation energies were 7 mJ at the two lower wavelengths and 10 mJ at the higher wavelength. Irradiance was

approximately 0.2 GW/cm^2 in each case. With an excimer laser at 0.308 μm, however, the initiation energy jumped to 75 mJ (~0.15 GW/cm^2). The spot size was larger and the duration of the pulse was longer for the excimer.

RDX was also successfully initiated with the excimer laser at 0.308 μm [6] and a ruby laser at 0.694 μm [2]. No details on the RDX type were provided and no other initiations with RDX have been reported. Attempts at initiating pure HNS have so far failed [5,6] even with a SSA up to 13 m^2/g and irradiance of 10 GW/cm^2 [6].

Dopants provide varied performance modifications. The addition of up to 10% graphite does not decrease the irradiance threshold for HNS to below 5 GW/cm^2 [5] in the wavelength range 0.266 to 1.06 μm while Zr-doped PETN shows enhanced sensitivity to laser ignition at 1.06 μm [6]. One to two percent of carbon black has increased the sensitivity of PETN to long duration pulses (several ms) at 1.06 μm [3].

Explosives initiated by direct laser interaction often exhibit excess transit times (t_e) measured in the 100s of nanoseconds [5,6]. The t_e typically increases as the threshold initiation energy is approached. There is a similar trend for shock impact initiation of HE [10], although the t_es are significantly shorter. For direct laser initiation, a requirement for the explosive to undergo a deflagration-to-detonation transition (DDT) is cited as the reason for the long t_e [6].

At wavelengths > 0.355 μm, confinement provided increased sensitivity to laser ignition [5,6]. Ostmark [11] has demonstrated, for RDX and PETN, that the ignition radiant exposure reduces as the pressure increases for irradiation at 10.6 μm with greater than 1 ms pulse duration. Paisley [5] suggested that the need for confinement is related to the mechanisms involved in the initiation process. It was suggested that confinement is not necessary at 0.266 and 0.308 μm as PETN is a strong absorber of UV radiation. The possibility that photo-dissociation may occur as a result of this absorption was presented. At the longer wavelengths, the initiation was considered to be thermal in nature, with confinement assisting the growth of the detonation from the generated hot spots.

Renlund et al [6] have suggested that as the absorption band of PETN is approached, the depth of laser penetration is reduced and the surface of the explosive forms the confinement until convective burn is sustained. At that stage a transition to detonation may proceed. The justification for this proposal is that ignition is relatively unaffected by confinement at 0.308 μm, but that confinement does decrease t_e. Reduction in t_e may be possible by increasing the initiating pressure and thus removing the slow layer-by-layer deflagration stage of the DDT [6].

Perhaps the single most important aspect of direct laser initiation studies of HE has been the ability to probe the decomposition process in fine detail. RDX and PETN have undergone such investigations [11-13]. Micrometre sized craters have been observed on the surface of these HE samples following laser irradiation. Possible reaction pathways have subsequently been proposed [12,13].

4.1.2 Thin Film in Contact with Explosive

Figure 2 shows that the initiator consists of a glass window, a thin metallic coating on the inside of the window and the explosive adjacent to the metal. Under irradiation, the confined metal layer explodes, generating a shock that impacts the adjacent explosive. This approach is also known as the EBW mode [5].

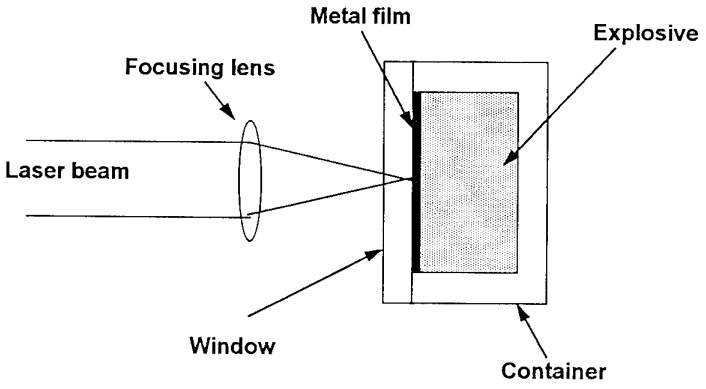

Figure 2: Schematic employed for laser initiation of HE in contact with a thin metallic foil.

The generation of the shock was investigated by Yang and Menichelli [2]. Twenty-six different materials, at thicknesses ranging from 0.004 to 1 μm, and confined between two glass slides, were studied. The results are summarised below:

(a) The stress pulse duration is approximately twice the laser pulse duration (FWHM).

(b) The peak stress increases linearly with radiant exposure to about 2 GPa at 14 J/cm^2 and a predicted 8 GPa at 56 J/cm^2. Sheffield and Fisk [14] report a pressure range of 1 to 10 GPa at 10 J/cm^2.

(c) The peak stress is independent of film material, in agreement with King [15].

(d) The peak stress is independent of film thickness except for metals with high thermal conductivity, and at low radiant exposures.

(e) The film thickness relevant to shock generation is of the order of several hundred Angstroms.

(f) Within the radiant exposure range investigated, approximately 10% of the energy is converted to stress energy. The remainder is either reflected, transmitted, or used for ablation or ionisation of the film.

If one of the confining glass slides is replaced by a porous explosive, the low impedance of the air tends to reduce the peak stress [2]. Local stresses generated within the explosive, however, may depend on the explosive morphology and the expansion velocity of the plasma rather than the presence of the air [2].

The high explosives PETN, RDX, tetryl and HNS have been evaluated by this initiation technique [2]. Using 1 μm thick Al film on the window, coarse grained (>100 μm) PETN at density 1.64 g/cm^3 showed a strong transition after a run distance of 24.5 mm. No detonations were observed for the coarse grained RDX. The maximum laser irradiance was approximately 9 GW/cm^2.

For fine grained (<40 μm) PETN at density 1.58 g/cm^3 and RDX at density 1.18 and 1.52 g/cm^3, detonations occurred over a much shorter distance than for the coarse grained material. In a number of cases there also appeared to be evidence of the formation of a super detonation wave. Results indicated that as the density of the explosive increased, so did the threshold irradiance. PETN was found to have a lower threshold irradiance than RDX; 1.4 GW/cm^2 compared to 5 GW/cm^2. Higher density RDX and low density Tetryl and HNS could not be detonated up to the maximum irradiance of 9 GW/cm^2.

More recently, Renlund et al [6] have induced detonation in high SSA PETN at density 1.2 g/cm^3 using a Nd:YAG laser at 1.06 μm and a 0.5 μm aluminized window. The irradiance required was about 1 GW/cm^2, which was slightly lower than required when using a clear window. The minimum t_e was 15 ns.

The effect of the film thickness on the initiation threshold energy has been investigated [2]. It was found that lower radiant exposures were required for thinner films. It was suggested that the thinner film forms a plasma in direct contact with the explosive. The hot plasma heats the adjacent explosive and the ensuing reaction is considered to be thermally based. Not all of the thicker film is converted into a plasma and therefore the hot plasma is separated from the explosive. In this case it was suggested that initiation is due to the shock wave generated by the original foil explosion. There appears to be incomplete understanding of the basic initiation phenomenon here and further investigation is warranted.

4.1.3 Flyer Plate Launch and Impact

The experimental design is similar to that shown in Figure 2. The difference is that the explosive sample is separated from the metal layer by an air gap (Figure 3).

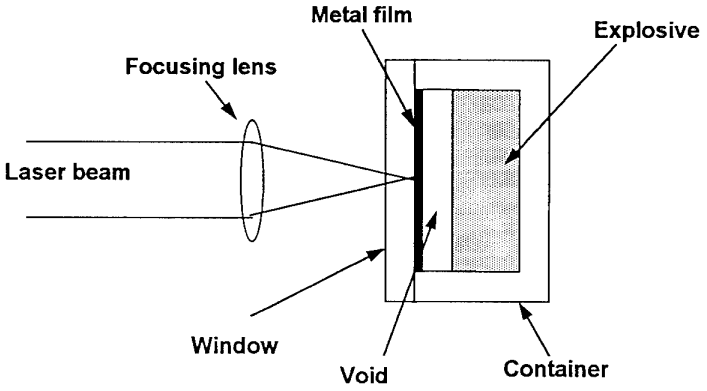

Figure 3: Schematic of the method employed for laser initiation of HE by ablation of a metallic foil to produce a flyer plate to impact the HE.

The concept of launching a laser-driven flyer plate was originally developed for fusion research [16-18] and for the study of high amplitude stress waves in materials [19-24]. In these studies, irradiances of up to 10^5 GW/cm^2 have been reported. Although such high irradiances are much greater than the ≤ 10 GW/cm^2 typically used to launch flyer plates at high explosives, the physics of the laser-metal interaction is basically the same and therefore not new.

The high intensity beam interacts with the metal to a skin depth dependent on the laser wavelength and the target material. For an Al target irradiated at 1.06 μm the skin depth is 5 nm. Krehl et al [25] show that to ionize and then heat such a small layer to a temperature of a few eV requires only about 10 mJ. Hence, at irradiances of several GW/cm^2 with sub-millimetre spot sizes and pulse durations < 10 ns, a very dense high-temperature plasma can be formed immediately after laser onset.

The density of the created plasma exceeds the critical density and therefore shields the target from further propagation of laser radiation at 1.06 μm. Additional laser radiation is then absorbed via inverse bremsstrahlung in a thin absorbing layer at the front surface of the plasma, where the plasma frequency is close to the laser frequency, and by non-linear parametric instabilities in regions where the plasma density is greater than the critical density [26].

During laser irradiation of the metal target, the created plasma expands adiabatically sending a shock into the remaining target material [16]. Several models have been developed to predict the laser/material interaction [16,19,27,28]. Ripin et al [16] have shown that the ablated plasma provides a thrust much like a rocket and that the initial

motion may begin as early as 8 ns prior to the laser pulse peak, although as the radiant exposure decreases, the initial motion begins later in the laser pulse cycle [29]. The thrust or blow-off velocity continues to increase as the peak is approached. The velocity changes of the target material have been observed to follow this trend [14,16].

For thin targets, when the displacement and the diameter of the accelerated foil are almost equal, the ablation is not strictly one dimensional due to lateral heat conduction [16]. It appears that laser energy is being transported to un-irradiated regions of the target adjacent to the irradiated region. The consequence of this is that the effective diameter of the ablated material is increased beyond the laser spot size and the thickness of the ablated material is reduced [16]. These edge effects may be important for the optimum design of the thin targets that are employed in the laser initiation of HE as a thinner than expected flyer plate will provide a shorter shock duration at impact with the HE. Shock duration is a relevant parameter in the shock initiation process.

The performance of the generated flyer plate has been the subject of many studies. Heavy tamping or confinement of the irradiated surface of the target can raise the generated pressure [24] from 1 GPa to 10 GPa at 1 GW/cm^2 [19] and also increase the duration of the pressure pulse [30]. This leads to a flyer plate propelled to a higher velocity. Sheffield et al [7] have reported a 430% increase in velocity as a direct result of confinement.

Final plate velocity has also been found to be dependent on the square root of laser radiant exposure [29] for radiant exposures >10 J/cm^2. With this knowledge, a simple kinetic energy relationship has been derived [29] that relates peak flyer velocity to the inverse square root of flyer plate thickness. This model is valid for flyer plate thicknesses <66 μm and diameters <1 mm [31]. At radiant exposures of approximately 25 J/cm^2, reducing the pulse duration increases the peak velocity further [29], although at medium and high radiant exposure the peak velocity becomes insensitive to pulse duration [32]. Pulse duration has a much greater effect on the flyer plate acceleration [29]. The reason for the modest increases in peak velocity as the pulse duration decreases is related to a limitation on the rate at which the laser energy can be coupled into the kinetic energy of the flyer plate [31]. A maximum coupling efficiency of about 40% was achieved for a pulse width of 4 to 8 ns [29].

In the laser initiation of HE, the launched target ultimately impacts a HE sample. Initiation of the explosive is therefore achieved by shock impact. Target velocity non-uniformities which may be due to target mass and laser irradiance non-uniformities, and hydrodynamic instabilities [17], can affect the response of the HE to the flyer plate impact.

PETN at density 1.4 g/cm^3 and fine particle size HNS at density 1.6 g/cm^3 have been initiated using laser-driven flyer plates (Nd:glass laser at 1.06 μm) [7]. The Al flyer plates were 66 μm thick and impacted the HNS at a velocity of about 2.5 mm/μs. Beam spot size was 1.5 mm, pulse width and irradiance were 16 ns and 11 GW/cm^2, respectively.

Smaller sized flyer plates (<1 mm in diameter and <10 μm thick) have been launched to velocities in excess of 5 mm/μs and with a high degree of planarity [8, 33, 34]. This performance was achieved by modifying earlier techniques [7, 14] by physical vapour deposition of the metal layer onto a UV-fused quartz substrate to provide solid tamping. The generated flyer plate diameters of 400 to 1000 μm were much greater than the <10 μm target thickness that was employed. In this instance, edge effects appeared to have no effect on the planarity of the flyer plate.

The peak velocity of the flyer plate was enhanced by depositing a dielectric layer (<0.25 μm) within the metallised deposit. The laser ablation stops at the dielectric layer thus controlling the actual flyer plate thickness. It is claimed that these modifications result in efficiency (kinetic energy of the flyer plate/laser energy on target) of approximately 50%. A further modification places the metallic target directly onto the tip of an optical fibre [29, 31, 34]. This approach forms the first step in advancing laser-driven flyer plates from a laboratory curiosity to a potential fuze application.

Fine grained HNS of SSA ~14 m^2/g and density near 1.6 g/cm^3 has been successfully shock initiated with laser-driven flyer plates. The actual irradiance was not specified, although it would appear to be <4 GW/cm^2 at 1.06 μm [8]. The flyer plate velocity was ~ 1.8 mm/μs providing an impact pressure of ~ 8 GPa and a shock duration of <1 ns.

It is interesting to compare the different threshold conditions for electrically initiated flyer plates and laser-driven flyer plates. Although the pressure at impact is slightly higher for the laser-driven flyer plate, the pulse width is more than an order of magnitude shorter [35]. This may indicate that the initiation criterion [36] is more heavily weighted in favour of the pressure than the shock duration for short duration shock initiation.

Characterising the velocity of the flyer plate is an important aspect in the understanding and implementation of laser initiation of explosives. Laser-driven flyer plates possess rapid acceleration ($\sim 10^{10}$ m/s^2) and achieve 90% of peak velocity in about 20 ns [8]. Standard VISAR [36] techniques cannot be employed to measure these velocities accurately [37]. In a traditional VISAR the photomultipliers and the digital recorder limit the time resolution of the measurement system. If the VISAR data is recorded on a streak camera the enhanced system known as ORVIS [37,38] provides improved temporal resolution, and accurate acceleration and velocity measurements of laser-driven flyer plates can be obtained.

4.1.4 Summary

By adjusting the density, the purity and the SSA of the explosive and the wavelength of the laser it is possible to initiate a range of high explosives by various laser initiation techniques. Adjusting the density and the purity of the explosive may, however, change the sensitivity of the modified explosive. This is not acceptable when the aim is to provide a more robust and safer fuze. In addition, explosives qualified for use in in-

line fuzes are limited by MIL STD 1316D. For practical fuzes the explosive of choice is HNS.

Precision timing, fast response, reduced electromagnetic vulnerability and low sensitivity of the initiating explosive are requirements for a modern fuze. The possibility of porting light to various initiation sites via optical fibres provides added versatility. It is apparent that both direct laser initiation and laser initiation via thin films in contact with explosives are unacceptable for incorporation in modern fuzes as neither can reliably initiate HNS. The production of laser-driven flyer plates that shock initiate the acceptor explosive, however, has been shown to successfully detonate HNS promptly. Presently, the only viable approach to laser initiation of HE in a fuze is therefore via laser-driven flyer plates.

Currently the size, cost and energy requirements of suitable lasers are too great for incorporation in all but the most expensive systems. Future laser developments will ensure that laser initiation will become a practical fuzing option. It is considered, however, that laser initiation will not become the only fuzing option and that slapper detonators will be an alternative. The selection will depend on the specific fuze requirements.

4.2 Laser Ignition of Pyrotechnics

Studies into laser initiation of pyrotechnics have tended to be directed in two major areas. Firstly, measurement of the sensitivity of the pyrotechnic material to laser energy (specifically the effects of the optical, thermal and physical characteristics of the material) including theoretical modelling. Secondly, the design and testing of practical laser initiation systems.

Laser studies of pyrotechnic compositions have been conducted with a variety of lasers including Ruby, Nd:YAG, CO_2, Nd:Glass, CW argon ion, laser diodes and pyrotechnically pumped Nd:Glass rods. At the same time, the range of pyrotechnic compositions studied has been broad, encompassing typical igniter compositions such as B/KNO_3, $Zr/KClO_4$ and $TiH_x/KClO_4$ as well as delays, coloured smokes, decoy and illuminating flares and thermites.

4.2.1 Sensitivity of Pyrotechnics to Laser Energy

One of the first papers to appear on the ignition of pyrotechnics using a laser was that of Menichelli and Yang [39]. They ranked the sensitivity of several common pyrotechnic compositions according to the laser energy density required to initiate them (Table 1). Free running pulsed Ruby and Nd lasers were used but their maximum output energy was only 15 J. They attempted to study the effect of some of the composition physical variables such as particle size and loading density on the ignition

threshold but the results were inconclusive. A similar inconclusive result was recorded for the effect of the laser pulse duration. However, their results were important as they showed that the laser ignition process was purely thermal in origin. This confirmed earlier work by Brish et al [40,41] who showed that the laser ignition of explosives was a thermal process and was not due to photochemical, electrical or light impact mechanisms.

Table 1: Order of ignition sensitivity of materials to laser energy (uncorrected for sample reflectivity) [39].

Order	Material	Average energy density to initiate,* J/in^2
1	Zr-KCl O_4	8.2
2	Lead styphnate	8.4
3	SOS-108 (neodynium)	12.8
4	SOS-108 (ruby)	13.8
5	Delay mix 176	14.1
6	Boron pellets (B/KNO_3)	19.9
7	Delay mix 177	21.0
8	Polyvinyl alcohol lead azide	21.9
9	Lead azide (dextrinated)	28.5
10	ALCLO No. 1 lead	44.0
11	ALCLO No. 2 iron	51.2
12	Mg/Teflon	73.0
* Energy density value is the mean value of all the conditions tested		

Magnesium/Oxidant Compositions

Holst [42] was one of the first to use a CO_2 laser (10.6 μm) to study the ignition of pyrotechnic compositions. A 1 kW laser was used to measure the time to ignition (t_{ig}) of a tracer composition for quality control purposes. The composition was based on Mg/$Sr(NO_3)_2$ primed with an igniter composition Mg/BaO_2/graphite/calcium resinate. With a 1s pulse duration (giving 350 W/cm^2), t_{ig} decreased with increasing pressing load i.e. composition density (Figure 4). This was contrary to what thermal ignition theory predicted. It was also noted that the sample surface roughness and reflectivity of the fuel/oxidants in the composition had an effect on t_{ig} but no results were presented.

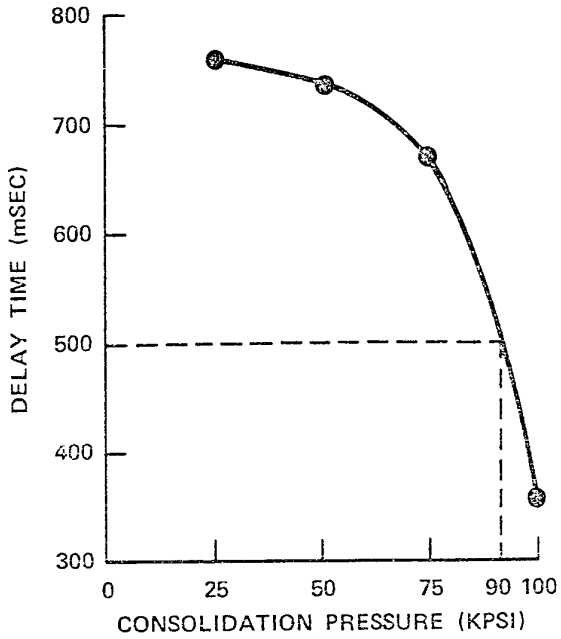

Figure 4: Effect of consolidation pressure on the delay time to ignition for Mg/BaO_2 based pyrotechnic compositions [42].

Oestmark et al., in several papers [43,44,45], examined some of the physical factors affecting the laser ignitability of Mg/BaO_2 and $Mg/NaNO_3$ compositions. In [43] a 300 W CO_2 laser was used to measure the critical energy density necessary to ignite a $Mg/NaNO_3$ sample at various pre-set pulse durations by varying the energy incident on the sample. The results showed that the total sensitivity for the material was defined by two ignition regimes (Figure 5). At short pulse durations, sensitivity was characterised by a threshold ignition energy density but at long pulse durations the ignition was characterised by a threshold ignition power. They used classical thermal ignition theory to develop two equations for the ignition power and the ignition energy:

$$E_{ign} = \frac{\rho C_p}{\alpha}(T_{ign} - T_o) \qquad (1)$$

$$P_{ign} = 2\lambda\omega\sqrt{\pi}(T_{ign} - T_o) \qquad (2)$$

From equation (1), the ignition energy was characterised by the internal properties of the material (heat capacity, thermal conductivity, etc), whilst from equation (2) the threshold power was dependant on sample area, and internal and external parameters of the sample. For $Mg/NaNO_3$, the threshold energy was approximately 2.1 J/cm^2 and the threshold irradiance was approximately 100 W/cm^2.

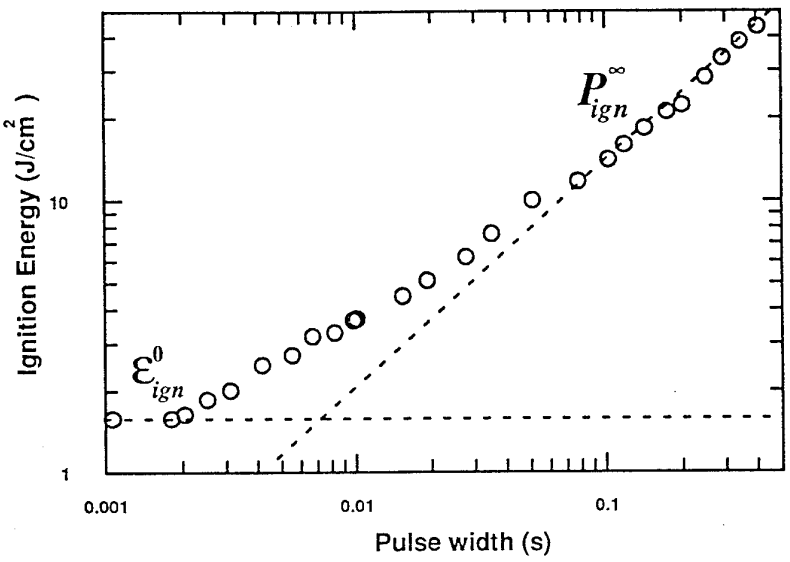

Figure 5: Ignition energy versus pulse width for $Mg/NaNO_3$. Observe the two ignition regimes: one for long pulses and one for short pulses [43].

In [44] Oestmark used the same 300W CO_2 laser to study the effect of changes in the particle size of sodium nitrate and type of magnesium powder in $Mg/NaNO_3$ and Mg/BaO_2 compositions. The laser spot size was 1.8 mm diameter, and the pulse duration was fixed at 43 ms. They found that the ignition energy increased with particle size (Tables 2 and 3) and attributed this to either changes in the thermal conductivity or change in the pathway in the mass transport process associated with ignition. They proposed that the effect of the different magnesium powders was due to small variations in κ (thermal conductivity) and the catalysis effects of MgO on the decomposition of the oxidiser.

Thermite Compositions

Thermite compositions were studied by Chow and Mohler [46,47] using a 60 W CO_2 laser with a spot size of 1 mm. They determined that the relationship between t_{ig} and laser irradiance was given by:

$$t_{ig} = \rho^2 q_0^{-m} \qquad (3)$$

where ρ is the sample density and q_0 is the incident laser irradiance. For Al/Fe_2O_3, values for m were between 1.2 and 1.4 and for Ti/2B m was 1.8. At a laser power of 25 W the time to ignition of Al/Fe_2O_3 was 42 ms. They noted that thermal ignition theory predicts values of m < 2.0 for propellants. They also noted that samples containing flake aluminium were difficult to ignite due to their higher thermal conductivity and high reflectivity.

Table 2: Threshold ignition energy for $Mg/NaNO_3$ pyrotechnic compositions for different particle size $NaNO_3$ (pulse duration 43 ms, spot size 3.6 mm) [44]

Particle Size (μm)	E_{ign} (J)
< 38	2.49 ± 0.09
38-45	2.83 ± 0.04
45-63	2.94 ± 0.09
63-90	3.08 ± 0.13
90-125	3.11 ± 0.14
125-180	4.16 ± 0.09
180-355	4.62 ± 0.14

Table 3: Threshold ignition energy of $Mg/NaNO_3$ for different types of magnesium powder (pulse duration 43 ms, spot size 3.6 mm) [44]

Type of Magnesium	E_{ign} (J)
Mil-P	3.08 ± 0.13
NKA 4629	3.44 ± 0.10
Microw-16.2	4.96 ± 0.06

Ti, TiH_X or Zr Fuelled Compositions

Many high reliability 1A/1W igniters use a pyrotechnic composition based on $Ti/KClO_4$ or $TiH_X/KClO_4$ pressed onto the bridgewire. As lasers represent an alternative to 1A/1W devices, much work has been carried out on the ignition of these compositions using lasers.

Holy [48] used a CW argon ion laser (514.5 nm) to study the ignition of $TiH_X/KClO_4$ (33:67) for x= 0.2, 0.65 and 1.65. As this set of experiments was designed to closely model hot wire devices, the spot size was set to 66 μm (approximate bridgewire diameter) and the pulse duration was set to 3 ms (approximate ignition time in hot wire devices). The energy of the laser was varied to determine the threshold energy and threshold power for ignition. The samples were tested under a pressure of 0.79 MPa of argon gas (Table 4).

Table 4: Threshold ignition power and energy for TiH_x /$KClO_4$ in 0.79 MPa argon (pulse duration 3 ms) [48]

x	Power (mW)	Energy (μJ)	Centre Power Density (kW/cm^2)	No. Samples
0.2	184.5 ± 2.5	554 ± 6	10.8	5
0.65	289 ± 2	866 ± 8	16.9	3
1.65	219.5 ± 7.5	657 ± 23	12.8	3

Holy found that increasing the laser power beyond the threshold required for ignition had little effect on the time to ignition. He did point out that the power levels recorded were low and that ignition was only achieved by having a very small spot size, thus ensuring a high irradiance. The irradiance was of the order of 10 kW/cm^2 at the beam centre. The ambient pressure also had a large effect on the ignition process; as the pressure increased from 0.45 MPa to 2.9 MPa, the time to ignition decreased and the ignition process became "smoother" and more reliable. The total light output of the reacting composition also increased significantly with ambient pressure.

Jungst et al [49] also studied the ignition of Ti/$KClO_4$ but used a 1 W laser diode (820 nm) coupled to a fibre optic. They found that a minimum power was required for ignition (0.35 W) and that increasing the power resulted in a reduction in the ignition energy. This resulted in an ignition energy/power map (Figure 6). These results confirmed the relationship between power and energy outlined by de Yong and Valenta [50] for Zr/$KClO_4$ and many other pyrotechnic compositions (Figure 7a and 7b). Kunz et al [51] also defined two ignition regions for Ti/$KClO_4$ depending on the pulse duration. At long pulse durations and low power levels, ignition was governed by the rate of heat loss from a critical volume in the composition. For shorter pulse durations when the rate of energy delivery (power) was high, ignition occurred as long as a minimum level of power was delivered. Jungst et al [49] also showed that the threshold ignition power increased with sample density and that the laser spot size was critical in determining the threshold energy and power levels. The greater the fibre optic diameter, the lower the threshold power density and the greater the threshold energy required for ignition (Figures 8 & 9). They found that for Ti/$KClO_4$, ignition only occurred when the fibre optic diameter was less than 200 μm. This could lead to a trade off in the design of practical systems - large fibres increase the coupling efficiency between the diode and the composition and enable low power diodes to be used but larger fibre diameters increase the ignition energy thresholds.

Further studies of TiH_X/$KClO_4$ compositions [52] confirmed that for samples in unsealed holders,the ignition power decreased with increasing pressure (Figure 10), increasing laser pulse duration (Figure 11) or increasing laser spot size (Figure 12). At low pressures there was also a clear difference between the ignition power requirements for a sample in nitrogen, argon or helium gas. In sealed holders, the threshold ignition power increased with increasing beam diameter and increasing hydride value (Table 5).

The nature of the surface of the composition (reflectivity which is a function of roughness, particle size, pressing load etc) was also shown to be critical to the energy and power thresholds which verified the earlier work of [46,47]. Holy [48] noted that for these compositions, their surface reflectivity noticeably decreased within microseconds after irradiation with the laser; this should make the sample more effective in absorbing the laser energy. Ewick et al [53] studied the effect of pressing load on the ignition energy and found that as ρ increased from 1.6 g/cm^3 to 2.2 g/cm^3, energy increased from 2.6 mJ to 3.5 mJ.

The use of additives to alter the ignition behaviour of Ti/$KClO_4$ compositions was tested by Ewick et al [54] using a Nd:YAG laser and pulse duration of 20 ms. The results showed that the addition of graphite at levels up to 5% had no effect on the threshold ignition power. It was proposed that the cause of this "negative" result was that the addition of the graphite did not significantly change the visual appearance of the composition surface. This result was not supported by the work of Kunz et al [51] who reported that the addition of only 0.5% of graphite to a Ti/$KClO_4$ composition resulted in an increase in the minimum ignition energy from 2.6 mJ to 3.2 mJ. It was proposed that this was due to the graphite acting as a heat sink, increasing the thermal conductivity of the composition and promoting the transfer of heat away from the $KClO_4$ particles. As a secondary explanation, the graphite also acts as a diluent so that a smaller effective area of titanium particles are exposed to the incident laser light. This is important as the highly absorbing materials at the laser wavelength used (830 ± 10 nm) are the titanium particles. Ewick [54] used a Nd:YAG laser operating at 1064 nm which may explain the lack of ignition dependence on the graphite dopant. An opposite result was recorded by de Yong and Valenta for Zr/$KClO_4$ where the minimum radiant exposure decreased from 3.3 J/cm^2 to 1.0 J/cm^2 with the addition of 1% graphite to the composition [50].

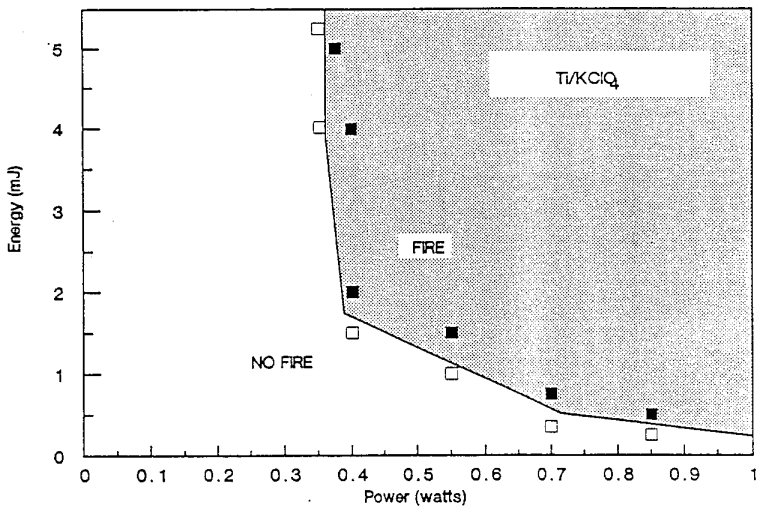

Figure 6: Threshold ignition energy and power for Ti/$KClO_4$ pyrotechnic compositions (pulse width 10 ms, 100 μm fibre optic) [49].

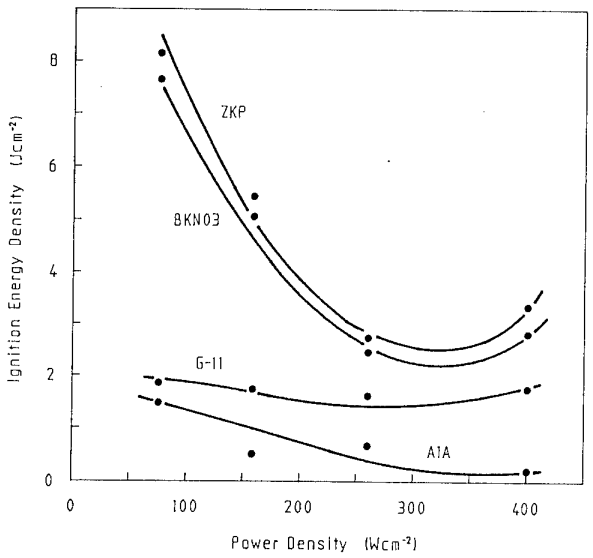

Figure 7a: Variation in the ignition energy with incident power for several pyrotechnic compositions (pulse width 100-200 ms) [50].

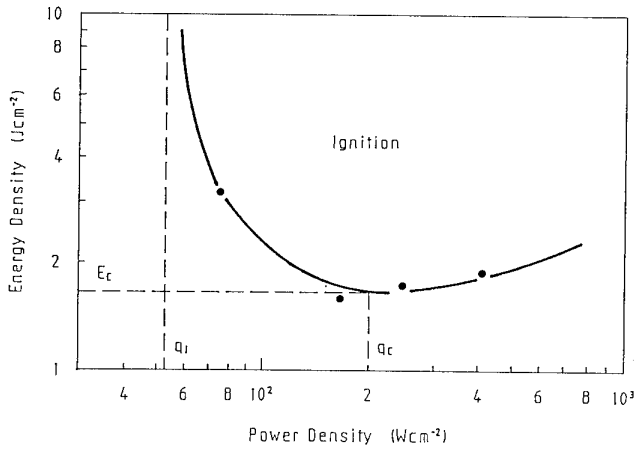

Figure 7b: Relationship between laser ignition radiant exposure (energy density) and irradiance (power density) for pyrotechnic compositions; q = minimum irradiance, E_c = minimum radiant exposure [50].

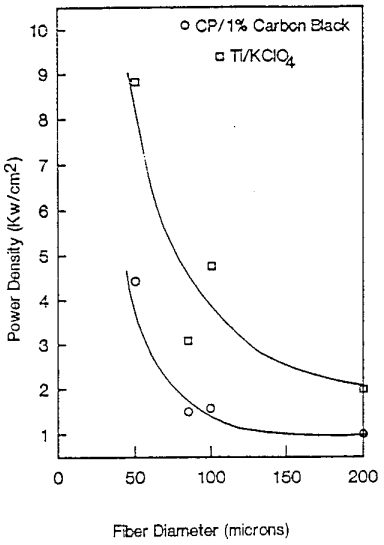

Figure 8: Variation in the threshold irradiance (power density) with fibre diameter for $Ti/KClO_4$ pyrotechnic composition (pulse width 12 ms) [49].

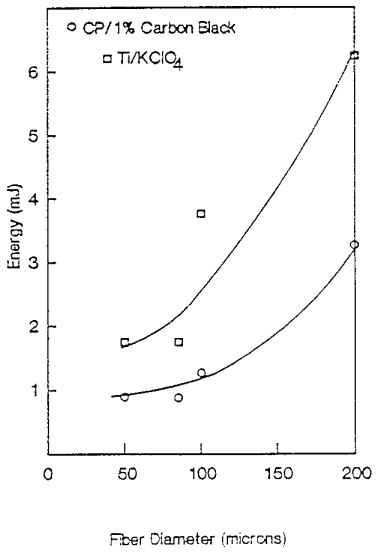

Figure 9: Variation in the threshold ignition energy with fibre diameter for $Ti/KClO_4$ pyrotechnic composition (pulse width 12 ms) [49].

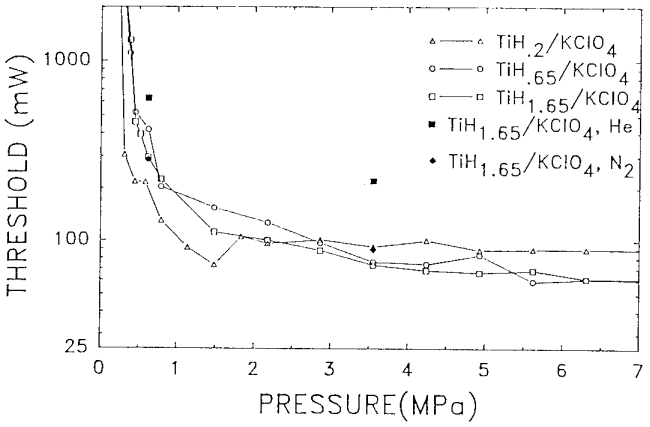

Figure 10: Change in the ignition power threshold for $Ti/KClO_4$ as a function of pressure and the type of gas (pulse width 3 ms) [52].

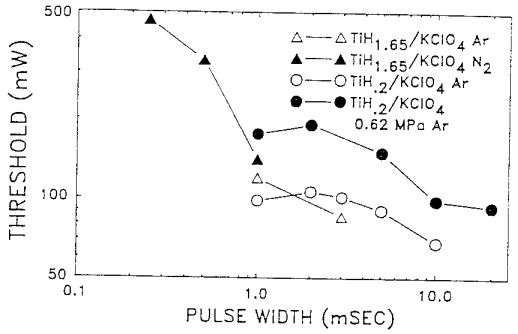

Figure 11: Variation in the threshold ignition power with laser pulse width for $TiH_x/KClO_4$ pyrotechnic compositions (spot size 65 μm) [52].

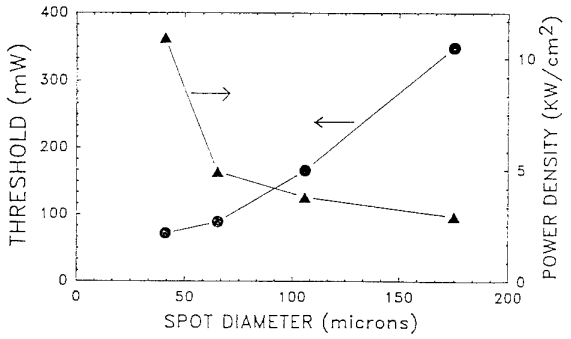

Figure 12: The effect of changes in the laser spot size on the threshold ignition irradiance (power density) and threshold ignition power for $TiH_{1.65}/KClO_4$ in 2.9 MPa argon [52].

Table 5: Threshold laser ignition power in a sealed windowed device for TiH_x /$KClO_4$ (pulse duration 20 ms) [52]

Sample	Beam Diameter (μm)	Threshold Power (W)	Central Power Density (kW/cm^2)
$Zr/KClO_4$ / Viton/Graphite	60 125	0.20 0.47	14.1 7.7
$TiH_{0.2}$ / $KClO_4$	60 125	0.40 0.72	28.2 11.7
$TiH_{1.65}$ / $KClO_4$	60 125	0.57 1.16	40.3 18.9

A detailed study of the effect of additives on the ignition of $Zr/KClO_4$ was made by Rontey [55]. He used a Nd:YAG laser and a short pulse duration of only 150 μs (4 mm spot size) to determine 50% (mean) ignition thresholds. The addition of graphite, carbon black, activated carbon, chromium oxide or boron to the $Zr/KClO_4$ composition resulted in the mean energy increasing in all instances. However, the use of glass spheres (10 μm and 25 μm diameter) in an attempt to focus the laser light to a multitude of points resulted in a significant reduction in the threshold radiant exposure from 1.7 J/cm^2 for 0% glass beads to 0.98 J/cm^2 for 5% glass beads, 0.82 J/cm^2 for 10% glass beads and 1.45 J/cm^2 for 20% glass beads.

Rontey also found that replacing the zirconium with hafnium increased the radiant exposure threshold from 1.1 J/cm^2 (0% hafnium) to 12.1 J/cm^2 (100% hafnium). He proposed that this was due to change in the thermal conductivity, the depth of absorption and reflectivity. The threshold ignition energy was also reduced by decreasing the sample density (changing the thermal diffusivity) or making the formulation fuel rich (greater light absorption and reacting surface area of the metal particles).

Teflon (PTFE) Based Compositions

de Yong and Valenta [50] measured the time to ignition at various pre set pulse durations for several types and physical forms of magnesium/Teflon/Viton (MTV) using a 400 W CO_2 laser. They found that there were real differences between the types of MTV examined, and ascribed these to the change in the particle size and surface area of the magnesium powders used and the variation in thickness of the Viton coating on the magnesium due to the change in the surface area. Typical results are shown in Figure 13. The formulations were ranked according to their minimum radiant exposure and MTV, at approximately 13 J/cm^2, was significantly greater than many other pyrotechnic compositions (Figure 7). At irradiance levels of 200 W/cm^2 the time to ignition for MTV is approximately 60-70 ms.

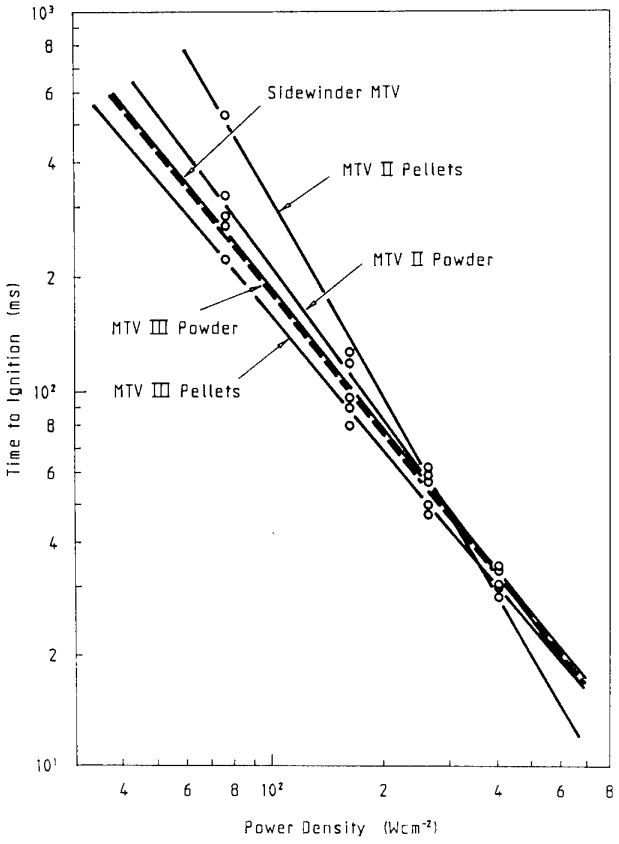

Figure 13: Relationship between time to ignition and the laser irradiance (power density) for several MTV compositions [50].

Fetheroff et al [56] studied the ignition behaviour of magnesium/Teflon and boron/magnesium/Teflon compositions (which are similar to some rocket motor igniter compositions) and examined the effect of the addition of boron on ignition and burn rate. Their results showed that as the percentage of boron increased, the time to ignition decreased; at 700 W/cm^2, t_{ig} decreased from 70 ms at 0% boron to 10 ms at 10% boron and approximately 2 ms at 35% boron. This result was thought to be due to the high absorptivity of boron and the decrease in thermal diffusivity with increasing boron content, which resulted in a concentration of energy at the sample surface.

Holy et al [52] showed that the ignition threshold for magnesium/Teflon compositions decreased with decreasing pellet pressing load and with increasing gas pressure (Table 6).

Table 6: Ignition thresholds for magnesium/Teflon pyrotechnic compositions (pulse duration 20 ms, spot size 65 μm) [52]

Sample	Pressing Pressure (MPa)	Gas Pressure (MPa)	Threshold Power (W)
Mg/Teflon	34.5	1.55	0.29
	82.7	1.55	>1.6
	82.7	5.64	1.2

Ramadhan et al [57] used a Nd:Glass laser to ignite MTV samples and measured the threshold radiant exposure at between 3.6 J/cm^2 and 6.1 J/cm^2; the variation was due to different particle size magnesium used in the compositions. They also multiple irradiated samples of MTV with the same irradiance and laser pulse duration until ignition occurred. It was noted that increased darkening of the sample surface occurred with each irradiation and that this would result in increased absorption of the radiation and increased likelihood of ignition.

Colored Smoke Compositions

Ignition of coloured smoke compositions has only been recorded by de Yong and Valenta [50]. They found that minimum radiant exposure was in the order 3.1 J/cm^2 to 6.9 J/cm^2, although the violet smoke composition recorded an unusually high threshold of 11.9 J/cm^2 (Table 7). The smoke compositions often showed erratic build up to ignition and combustion continued only as long as the sample was irradiated with the laser. The smokes ignited reasonably slowly with t_{ig} recorded at 200-300 ms at laser irradiance of 200 W/cm^2.

Delay Compositions

Only limited studies have been conducted on delay compositions. Si/Pb_3O_4 and Sb/$KMnO_4$ delays were studied by Brochier [58] using a Nd:Glass laser with a 200 μs pulse duration. The radiant exposure for 50% ignition were measured to be 725 mJ/cm^2 and 3.5 J/cm^2 respectively.

de Yong and Valenta [50] and Fetheroff [59] both studied T-10, a B/$BaCrO_4$ delay composition. They both measured the time to ignition as approximately 10 ms at a laser irradiance of 200 W/cm^2, although Fetheroff noted that there was significant batch to batch variability in the time to ignition at low irradiance (80-200 ms at 75 W/cm^2).

Table 7: Minimum laser ignition radiant exposure (energy density) for several pyrotechnic compositions [50]

Composition	Laser Initiation Energy Density (J/cm^2)
Ignition Compositions	
A1A	1.2
T-10	1.7
G-11	2.3
B/KNO_3	3.0
$Zr/KClO_4$	3.3
Smoke Compositions	
SK 354	4.9
SK 338	3.7
SK 356	3.9
USV	11.9
USG	4.0
USY	2.5
USR	3.1
UKB	3.1
UKG	3.1
UKD	3.8
UKR	3.9

Fetheroff et al [59] showed that the time to ignition was dependant on the laser irradiance, the rate of heat diffusion from the sample surface into the sample and the chemical heat generation:

$$\partial T/\partial t = q_{rad} + q_{diff} + q_{chem}$$

They showed that as boron is added to a $B/BaCrO_4$ composition (up to 3%), the time to ignition increases because q_{diff} dominates (thermal diffusivity of boron is almost two orders of magnitude > that for barium chromate). But at boron contents >15%, q_{chem} dominates and the time to ignition decreases. The luminous output from the ignited composition was also examined to study any pre-ignition process.

de Yong and Valenta [50] studied the effect of changes to the sample density (pressing load) for the T-10 delay composition and found that the time to ignition decreased as the density increased (Figure 14). This behaviour was most pronounced at low laser irradiances and was similar to that observed by Holst [42].

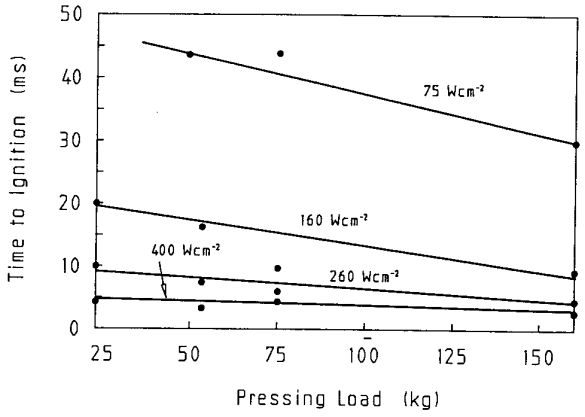

Figure 14: Effect of pressing load on the time to ignition of T-10 delay composition [50].

Other Compositions

Kordel [60] studied the ignition of several common pyrotechnic igniter compositions; B/KNO_3 and black powder using a Nd:YAG laser. He confirmed the results of [46], where at short pulse durations ignition was characterised by an energy threshold and at long pulse durations by a power threshold. The effect of spot size was also studied; as the diameter decreased the ignition energy decreased (Figure 15), which confirmed the earlier work on $Ti/KClO_4$ [50].

de Yong and Valenta [50] used a 1 kW CO_2 laser and found a similar dependence on irradiance for many other pyrotechnic compositions including coloured smokes, delays and igniter compositions. They proposed that the ignition behaviour of pyrotechnics could be characterised by a minimum or critical energy and a critical irradiance (Figure 7b). They compared the minimum radiant exposure for ignition for a range of compositions and found that some coloured smoke compositions and delays had ignition radiant exposures similar to igniter compositions (Table 7).

Refouvelet et al [61] determined the laser ignition energy levels using a Nd-Glass laser (1.6 mm spot size) for several igniter compositiions (Al/CuO, $Zr/KClO_4$) and percussion primer compositions ($KClO_4/Sb_2S_3$/lead thiocyanate). The work was designed to prove the feasibility of a laser initiated device for weapons of any calibre.

Brochier [58] studied both $Al/KClO_4$ and Zr/Cr_2O_3 compositions and showed that the 50% ignition energy increased as the pressing load increased from 70 MPa to 180 MPa.

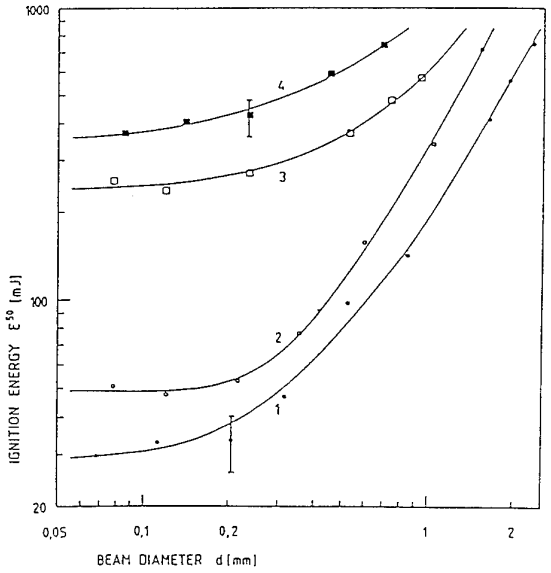

Figure 15: 50% ignition energy versus laser spot size for several pyrotechnic compositions (pulse width 50 ms): 1. NKP-S-5360, 2. B/KNO_3 , 3. S 2956, 4. Black powder [60].

4.2.2 Modelling Laser Ignition of Pyrotechnics

Modelling the laser diode ignition process was first attempted by Ewick [62]. He used a 1-D heat transfer equation to model the ignition of Ti/$KClO_4$ and CP:

$$\rho c \, \partial T/\partial t = k \, \partial^2 T/\partial x^2 + q$$

where ρ is the sample density, q is the heat generation value, c is the heat capacity. It was observed that the calculated results for the time to ignition were very dependant on the optical absorptivity value chosen. The model also showed that the ignition threshold decreased with increasing temperature and that there were significant differences between the nature (quartz or sapphire) and the thickness of the windows used to hermetically seal the powder. The main disadvantage of using a hermetic window was beam divergence which increased the spot size on the sample, reduced the power density and increased the time to ignition .

Skocypec et al [63] used a 1-D theoretical model which included scattering of the incident radiation (reflectance and transmission) but agreement with experimental results was poor. It was proposed that this was due to the lack of accurate optical and thermal data on the compositions. However, the model showed that at high power

levels (>0.2 W, short pulse duration) radiative heat transfer dominated whilst at low power levels (<0.2 W, long pulse duration) conductive heat transfer was dominant. Therefore, the materials and the design of the laser igniter will be important for ignition at low power levels.

Ewick [64] subsequently refined his ignition model and developed a 2-D finite difference model based on the equation:

$$\partial^2 T/\partial r + (1/r)\,\partial T/\partial r + \partial^2 T/\partial z^2 + q/k = (1/a)\,\partial T/\partial t$$

The results showed that the ignition threshold increased with fibre diameter, was greater for shorter pulse durations and decreased with increasing temperature. The 2-D model matched the experimental data better than his earlier 1-D model [62].

Glass et al [65] developed a three flux radiation transfer model of the thermal response of a laser diode igniter and the results showed reasonable agreement with experimental data (Figure 16). It was proposed that the differences between the theory and the experimental results were due to the errors in the values used for parameters such as the thermal conductivity, heat capacity and extinction coefficient of the energetic material.

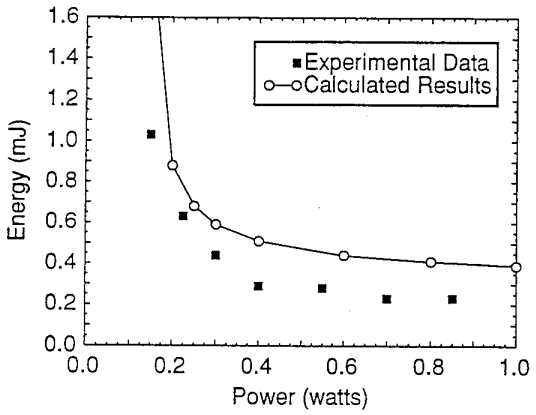

Figure 16: Calculated ignition threshold versus experimental results [65].

Oestmark [45] also attempted to model the laser ignition process using TOPAZ, a 2-D finite element computer model (simple heat transfer with first order Arrhenius kinetics). Although the ignition energy could be reasonably well predicted, the time to ignition was modelled poorly.

The development of mathematical models to predict laser ignition behaviour is well advanced but the models lack the required accurate physical parameters to reliably predict ignition behaviour.

4.2.3 Pyrotechnic Laser Ignition System Design

One of the earliest laser/fibre optic initiation systems which offered weight and volume effeciencies was studied by Kaminskii et al [66]. They used $Zr/KClO_4$ pyrotechnic compositions to optically pump an Nd laser rod. Using 1 gram of $Zr/KClO_4$, the maximum delivered energy was 0.5 J in an 18 ms pulse. Significant improvements were made by Yang et al [67] who used commercial zirconium/oxygen based photo-flashbulbs to pump the Nd:Glass rod. Effeciencies were significantly greater compared to the use of $Zr/KClO_4$ pyrotechnic compositions (Figure 17).

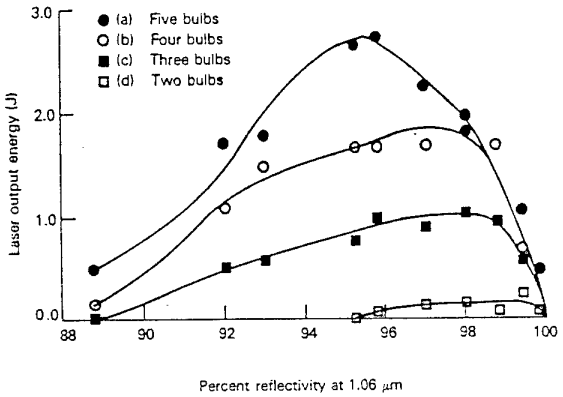

Figure 17: Relationship between laser output energy, number of flashbulbs and output mirror reflectivity [67].

In the late 1980s, several papers appeared on the application of solid state lasers and laser diodes to replace current hot wire devices. All approaches used fibre optics to transmit the laser radiation from the laser source to the pyrotechnic composition in the igniter.

Ewick et al. [54] initially used a Nd:YAG laser (pulse duration 20 ms) coupled to an igniter via a 125 μm fiber optic cable to determine ignition power thresholds for several igniter compositions (Table 8). Based on these results, prototype igniters were tested using a laser diode (830 nm) as the power source. For the BCTK composition the threshold energy was 648 mW at -65°F (18.3°C).

Jungst et al. also developed a sealed hermetic igniter using sapphire or soda glass windows [68]. Results for ignition of $Ti/KClO_4$ showed that the lowest ignition thresholds were measured using low thermal conductivity soda glass.

Table 8: Threshold laser ignition energy and power for several pyrotechnic compositions based on Ti/$KClO_4$/graphite (pulse duration 20 ms) [54]

Pyrotechnic Composition	Power (50% average) (W)	Standard Deviation (W)	Number of Tests	Energy (50% average) (mJ)
BCTK (B/$CaCrO_4$)	485	0.079	19	9.7
Ti/$KClO_4$	387	0.061	20	7.7
Ti/$KClO_4$/5% Graphite	384	0.060	20	7.7
Ti/$KClO_4$/2% Graphite	385	0.088	20	7.7
B/$KClO_4$	302	0.051	15	6.0

Petrick [69] proposed three practical laser ignition systems for energetic materials using fiber optics as the means of delivering the initial firing energy - direct fibre to material connection, laser light to an exploding foil and laser light to drive a slapper detonator type design. He noted that an optical window was needed to couple the laser light from the fibre optic to the sample. At short pulse durations the radiant exposure was the critical factor and the window and the air interface resulted in losses of up to 50% of the radiant exposure due to spreading of the laser beam.

Jungst et al [49] attempted to develop an optically ignited analogue to the current low energy hot wire igniter, DDT detonator, and actuators using a laser diode design. Three basic designs were examined (Figure 18):

1. In situ sealed pigtail of fiber optic for small devices;

2. Sealed fiber connector which ensures a small spot size at the powder interface but alignment is critical; and

3. Sealed connector with a sealed sapphire window; this removes the alignment problem but beam divergence becomes important. Addition of a reimaging lens system could overcome the problem.

Landry et al [70] proposed a laser initiation system based on optical fibres for aircrew escape systems. They studied the range of available lasers suitable for such a system and outlined a generic system (Figure 19). Based on the earlier work of pumped Nd rods [66,67], they described a prototype pyrotechnic laser initiation system that could be:

1. Mechanically operated single shot (6 zirconium flashlamps to pump the laser rod) producing 6 J for 30 ms;

2. Gas operated single shot (same as above);

3. Electrically actuated single shot (4 zirconium flashlamps to pump the laser rod), producing 2.1 J. If the output is split into two, each beam produced 1.7 J.

A typical design of this system, shown in Figure 20, was capable of initiating up to 16 initiators containing B/KNO_3 or up to 28 initiators containing CP. This is a large improvement on laser diodes that are typically only able to initiate a single CP initiator.

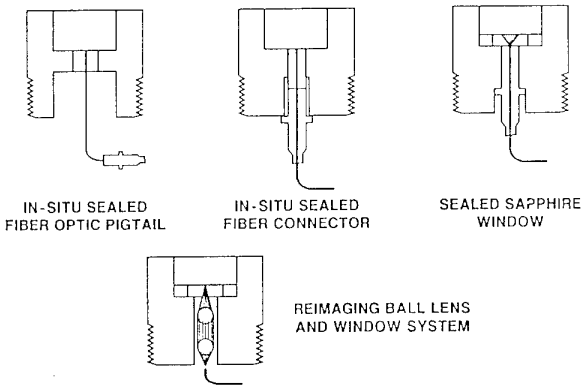

Figure 18: Design of three possible fibre optic/pyrotechnic powder interface concepts for a laser initiator [49].

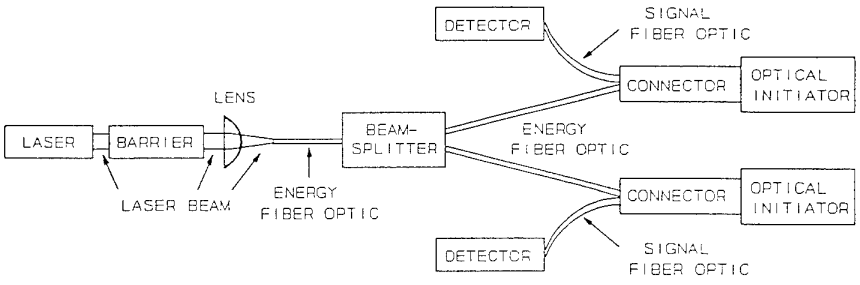

Figure 19: Prototype pyrotechnic laser initiation system [70].

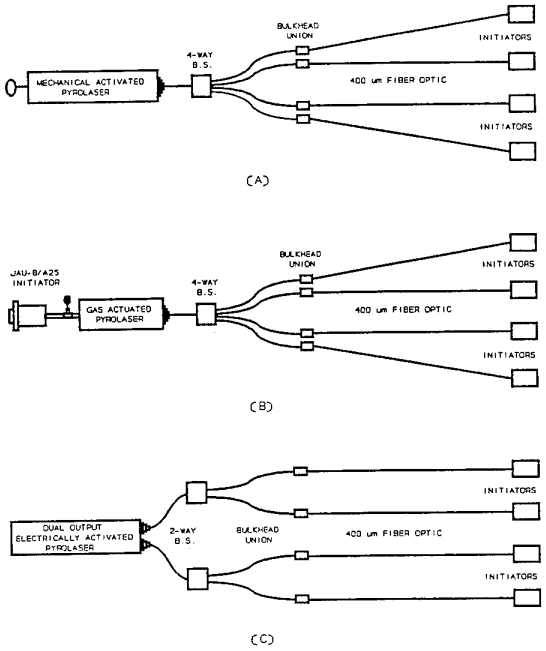

Figure 20: Breadboard design for (A) mechanical, (B) gas operated and (C) dual output electrically activated pyrotechnic laser ignition system [71].

Blachowski [72] further detailed the performance of this type of flashlamp pumped laser initiator (called a Laser Initiated Transfer Energy Subsystem - LITES). Seven flashlamps were used to pump a Nd doped glass rod (3% doping for maximum energy output) and the average output energy was 1.5 J. The output from the glass rod was taken to a bundle of thirty-seven 200 μm optical fibres and to a simple optical initiator containing $Zr/KClO_4$ or B/KNO_3/A1A compositions (Figure 21). Lasing of the rod commenced before the flashlamps reached peak light output (approximately 10 ms) and the laser pulse duration was 15 ms. The average energy delivered to the $Zr/KClO_4$ initiator was approximately 160 mJ and the time to ignition was approximately 7.5 ms. For the B/KNO_3/A1A initiator, the ignition time was 16 ms.

Ewick et al [53] carried out a reasonably comprehensive study on the factors affecting the ignition of a $Ti/KClO_4$, $TiH_x/KClO_4$ (x=0.65,1.65) initiator with a 0.25 W laser diode operating at 800-850 nm. The fibre optic was 100 μm in diameter and the pulse duration was 10 ms. The design of the test component is shown in Figure 22. For all three compositions at ρ=2 g/cm^3, the threshold ignition energy was between 2.8 mJ and 3.1 mJ; there was no statistical difference between the three compositions, in contrast to earlier results [48,52].

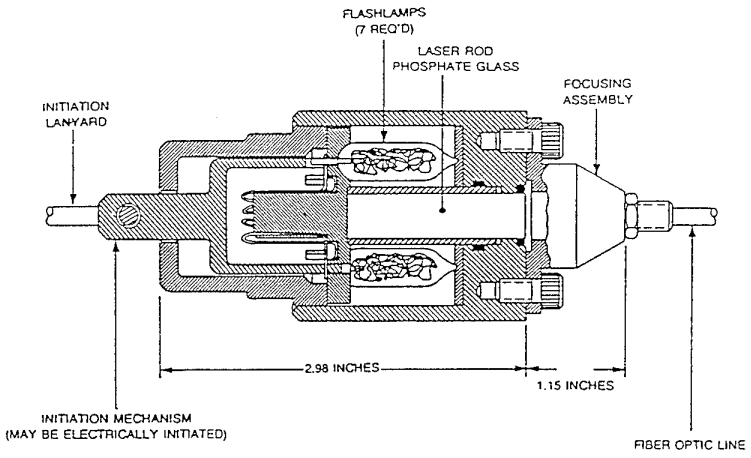

Figure 21: Design of the LITES mechanical actuation system [72].

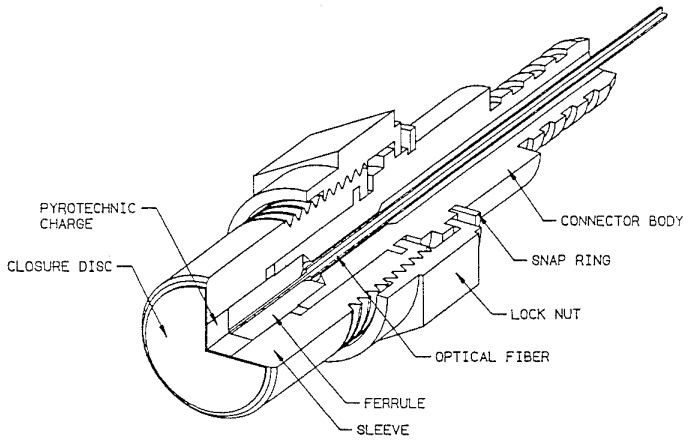

Figure 22: Laser diode ignited test component [53].

Since the ignition process is thermal in origin, the effect of the igniter construction was examined with respect to the thermal losses from different construction materials. The threshold energy decreased from 1.79 mJ with an aluminium ferrule to 1.51 mJ with a ceramic ferule. If a mylar disc was placed between the pyrotechnic powder and the fibre optic the ignition energy increased from 1.79 mJ to 3.58 mJ. The differences between these energies was proposed to be due to thermal conductivity differences between the materials. Changes in the ignition sensitivity from changes in powder density were confirmed for $Ti/KClO_4$ where the ignition threshold increased from

2.5 mJ at 1.6 g/cm^3 to 3.5 mJ at 2.2 g/cm^3. It was shown that using a graded index fibre rather than a stepped index fibre resulted in a concentration of the power closer to the centre of the fibre and a consequent approximate 30% lowering of the threshold energy. For Ti/$KClO_4$ this resulted in the ignition threshold being reduced from 2.9-3.3 mJ to 2.2 mJ. Combining all these features (ρ=1.8 gcm^{-3}, graded index fiber and mylar disc) the threshold ignition energy was reduced to 1.8 mJ.

Kramer et al [73] followed up on this work and reported that the major problem in developing a practical laser initiator was the hermetic seal of the fibre in the housing. If a window was used between the fibre and the pyrotechnic, the window must be sealed to a metal outer case with all the thermal expansion problems associated with dissimilar materials. High strength was only achieved with thick windows and this caused beam divergence and reduced radiant exposure to the powder. P glass was significantly better than sapphire windows due to its lower thermal conductivity and its lower refractive index which results in reduced beam divergence. If the fibre was sealed in a glass seal then sealed in a metal holder, leak tight crack free seals were only achieved through rigid control of the sealing process and problems could still occur due to the thermal expansion differences between the fibre, the glass seal and the metal holder.

Rupert et al [74] developed a laser ignited Zr/$KClO_4$ igniter for a 120 mm gun system. A Nd:YAG laser was used and the igniter initiated the bennite filled M83 cannon primer.

4.2.4 Mechanisms for Laser Ignition of Pyrotechnics

In [45] Oestmark et al. expanded on the work in [44] and established a mechanistic model of the pyrotechnic ignition process. A 250 W CO_2 laser was used along with high speed photography to visually study the reaction and ignition zones. From these studies the ignition mechanism of the Mg/BaO_2 composition was proposed to proceed in several steps:

1. BaO_2 decomposes producing oxygen;
2. Diffusion of the oxygen through the oxide layer of the magnesium particles;
3. Reaction between gas and solid - (single particle combustion); and
4. Growth phase (interaction with multiple burning particles).

The evidence for this mechanism came mainly from the lack of a pressure dependence of the ignition energy and the visual observation of a pyrotechnic hot spot before bulk ignition commenced.

For Mg/$NaNO_3$ composition, all the same steps are involved but an additional step occurs first - the $NaNO_3$ melts before it decomposes [45].

The observation of pre-ignition reactions by Oestmark [45] was also noted by Holy [48] for $TiH_x/KClO_4$ and by de Yong and Valenta [50]. Using a 1 kW CO_2 laser, it was found that for MTV compositions the response of the photodiode used to determine the moment of ignition often showed erratic pre ignition behaviour [50](Figure 23a and 23b). It was proposed that the photodiode was responding to localised hot spots on the surface of the sample but that the size of the hot spot formed was insufficient to progress to ignition. This theory was confirmed by the work of Ramadhan et al [57], using a Nd:glass laser with a pulse duration of 560 μs to ignite pellets of MTV and high speed cameras to view the ignition process. It was shown that the self sustaining fast reaction initiated at microscopic regions within the sample and that small hot spots formed in the sample before self sustaining ignition commenced. It was also shown that the exothermic reaction was between Mg and F_2 and that the ignition process was initiated at the Mg/Viton interface, but it was not possible to resolve whether ignition occurred in the gas or solid phase [57].

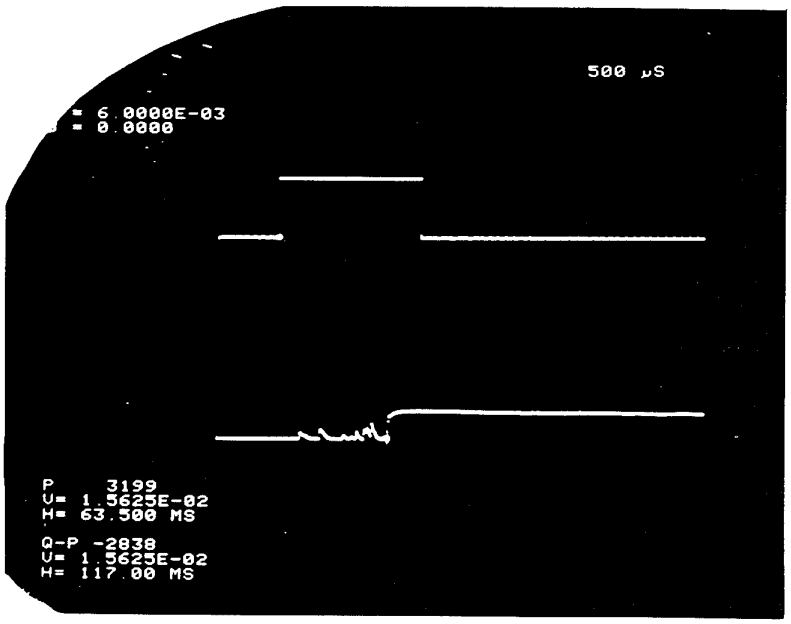

Figure 23a: Oscilloscope response for laser ignition of typical MTV composition [50]. Top trace is the laser pulse, bottom trace is the photodiode response showing pre-ignition behaviour followed by sustained combustion.

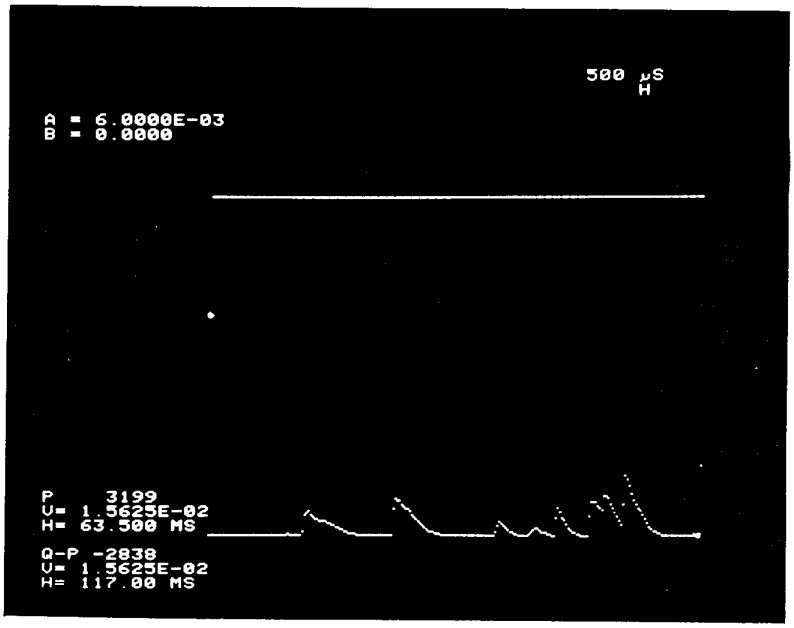

Figure 23b: Enlarged view of pre-ignition behaviour shown in Figure 23a.

4.2.5 Thermal Analysis

Temperature profiles of the surface of thermite compositions were measured by Chow and Mohler [46,47] using infrared thermography. The total heat content of the sample was calculated from the observed temperature distribution. These studies were extended to Ti/2B and Al/Fe_3O_4 compositions [75]. By measuring the temperature of the sample during irradiation, the activation energy of Al/Fe_3O_4 was calculated as 251 kJ/mole.

4.2.6 Summary

The use of lasers in initiation systems or as research tools with pyrotechnic compositions has developed significantly in recent years. Apart from the breadth of the research on variables affecting the laser ignition threshold for many pyrotechnic compositions, the design of practical initiation systems is at an advanced stage. Although systems utilizing expensive laser diodes may not quickly find many practical applications due to their high cost, systems such as the single shot flashlamp pumped laser igniter offers all the advantages at a much lower cost.

4.3 Laser Initiation of Propellants

Ignition is the first step in propellant combustion; it is a transient phenomenon leading to steady-state combustion. As the propellant sample is externally heated, there is an increase in the surface temperature and the build-up of a thermal profile. This leads to decomposition of the propellant with evolution of gaseous reaction products. The reaction products react exothermically with one another, giving rise to heat release which increases the gas-phase temperature and, consequently, the reaction rates themselves. With additional heating together with a concentration build-up of the gas-phase species, heat feedback from the flame to the burning surface occurs until a point is reached where the flame provides sufficient energy for self-sustained burning of the propellant; the external heat source is no longer necessary, and the ignition phase is complete. The sample has entered the steady-state combustion regime, and the rate of surface regression, i.e. the so-called burn rate, will be determined by the balance between the heat generated by, and heat feedback to, the burning surface.

In general, solid propellants in rocket motors are initiated by pyrotechnic igniter.

4.3.1 Laboratory R&D

In what follows, laboratory R&D activities involving laser ignition of propellants are reviewed with a view to obtaining an understanding about the technology involved.

It is important at this juncture to distinguish between the two different modes by which energy is transferred to the propellant surface. In radiative ignition, the energy flux to the surface remains constant while the surface temperature rises to a critical value associated with ignition. In conductive ignition, the surface temperature remains constant while the energy flux into the propellant decreases with time. For a specified ignition time, the surface temperature at ignition by conductive heat transfer is well below that at ignition by radiation.

4.3.2 Propellant Ignition Theories

Historically, theories of solid propellant ignition started to appear in the 1950s. The first paper by Hicks reported on numerical solutions where the propellants were treated as homogeneous reactive solids subjected to surface heating [76]. Double base propellants were considered as igniting due to solid phase exothermic reactions. This concept thus seemed to exclude composite AP propellants as likely candidates for ignition. Some excellent reviews have been published, notably by Price et al. [77], Brown, Anderson and Shannon [78], Kulkarni et al. [79], Kishore and Gayathri [80], and Hermance [81].

There are three principal theoretical models describing various physico-chemical processes of ignition. The models in general have been based on the principle of exothermic chemical reactions with external heat addition as necessary. They differ, and are classified, depending on the various locations and types of exothermicity. The three main theories are: the solid-phase reaction theory, the gas-phase reaction theory, and the heterogeneous reaction theory. The excellent review by Hermance [81] has critically discussed in detail these theories and provided a comprehensive summary of all the important work, in chronological order up to about 1978.

The Solid-Phase Reaction Theory

This theory, proposed by Hicks [76], suggests that exothermic chemical heating occuring in the propellant solid raises the surface temperature to the point of ignition. Ignition is governed by the temperature rise in the solid below the surface exposed to heat flux. The solid-phase models have been extensively studied numerically by Baer and Ryan [82,83], Bradley [84], and served as good foundation for a series of analytical papers by Williams and his colleagues [85]. The studies by Baer and Ryan [82] and by Bradley [84] considered pulsed radiant energy input and a go/no-go ignition criterion, and their results were interpretable in terms of ignition delay as a function of flux at constant pressure and as a function of pressure at constant flux.

The Gas-Phase Reaction Theory

The essence of this theory is that upon application of thermal stimulus, a propellant decomposes, producing gaseous fuels and oxidants that are transported away from the decomposing surface by diffusion and convection, while simultaneously participating in exothermic chemical reactions which may be affected by the composition and pressure of the external gas phase. The chemical reaction is limited by the amount of fuel/oxidiser mixing and the local temperature through an Arrhenius reaction of some specified order with respect to each reactant. According to this theory, the runaway heating conditions are achieved as a result of the gas-phase exothermic chemical reactions between the propellant constituents at a small but finite distance from the surface. Gas-phase reaction modelling work has progressed from the original numerical studies on pure fuels [86], to homogeneous propellants [87], and to heterogeneous propellants [88]. Radiation-stimulated, gas-phase ignition was studied numerically by Shannon and Deveral [89], Kumar and Hermance [88,90], and Kashiwagi [91], and analytically by Kindelan and Williams [92]

The Heterogeneous Reaction Theory

This theory states that the ignition process is controlled by the primary reactions between the gaseous decomposition products of the oxidiser and the solid organic binder which occur at or below the propellant surface. The heterogeneous reaction model has been studied extensively by numerical treatment by Bradley and Williams

[93], and by analytical treatment by Waldman and Summerfield [94], and Linan and Crespo [95].

4.3.3 The Ignition Map

The sequence of processes within an ignition event can be summarized [96] in the ignition map (Figure 24) which shows a plot of the logarithm of the radiant heating time against the logarithm of the irradiance. Consider a propellant subject to a fixed irradiance corresponding to the vertical line in Figure 24. At short times the rise in surface temperature will be insufficient to induce any significant reaction. If the radiant heating is terminated, the propellant will appear to be unchanged macroscopically. If instead the radiant heating is continued, the propellant surface temperature will rise to a value at which propellant gasification reactions will occur abruptly. This sudden change in behaviour defines the "first effect" or gas evolution boundary, denoted as the L_{1a} boundary. It is usually the result of chemical processes in the condensed phase and is pressure independent. The location and irradiance-dependent behaviour of this boundary has been described by thermal ignition theories [97,98]. Continued surface decomposition reactions give rise to gas evolution and heat release, which leads to IR signals being recorded. This denotes the boundary L_{1b}. This boundary is less precise than the L_{1a} because it depends on the sensitivity of the IR detection system. However, it is indicative of the onset of flame development in the gas phase. As irradiation continues, the next boundary L_{1c} is reached where the flame is substantially developed. Since the gas phase flame development is a continuous process that does not pass through sharply defined phases, the boundaries L_{1a} and L_{1b} only serve to elucidate the rate of flame development and its dependence on ignition parameters.

Continued irradiance leads next to a sharp boundary defined by the go/no-go nature of the test; this is defined as the self-sustained ignition line L_{1d}. When this boundary is crossed, removal of the radiation is followed by sustained burning of the propellant. Note that crossing the boundaries L_{1a} to L_{1c} does not assure continued burning after stopping the radiation. The position of L_{1d} is pressure dependent; it reflects the time of attainment of a gas phase flame that has steady-state flame characteristics. Models are available for predicting the location and behaviour of this L_{1d} boundary [87a,99]. In general, L_{1d} is the last limit encountered with increasing radiation time; any longer exposure would still lead to continued burning, although some exceptions were noted in which continued irradiation led the flame into a steady-state condition which is artificially forced to a higher rate by the external radiation, as compared to a steady-state value without radiation [100].

The sustained combustion of certain propellants, e.g., uncatalyzed double base propellants, cannot survive the disturbance caused by abrupt termination of radiation. When the radiation stops, the propellant extinguishes (line L_2) in much the same way as if it had been rapidly depressurized. This gives rise to the termination boundary L_2. Certain non-idealities, such as propellant transparency, could significantly affect this boundary [101].

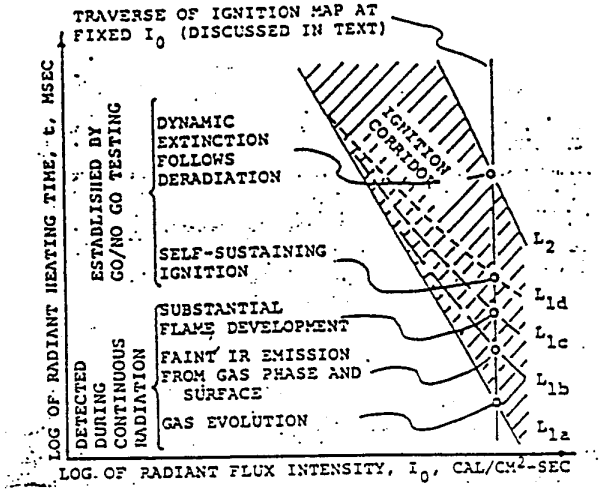

Figure 24: Detailed ignition map [96].

In general, the ignition map for many propellants is much simpler than that in Figure 24. The boundaries L_{1a} to L_{1d} may collapse to a single boundary L_1, and L_2 may not always exist [96]. The use of high pressure greatly simplifies the ignition behaviour in go/no-go testing; the ignition map reduces to a single line above which self sustained ignition ensues, i.e. the L_{1d} limit (self-sustained ignition) coincides with the L_{1a} limit (first gas evolution). The location and slope of this L_1 boundary are affected by three factors: surface reflection, in-depth extinction coefficient, and propellant reactivity [96].

A much more generalised depiction [102] of the ignition process is given in Figure 25. It defines three regions: the inert heating region, pre-ignition region, and self-sustained combustion region, which are separated by the first gasification curve and the go/no-go ignition curve.

The following example [103] demonstrates the consequence of events occurring during the ignition process of a sample of nitramine propellant. For a given irradiance (dotted line in Figure 25), a series of events take place at various time over which the sample is subjected to the irradiance. For some initial time, nothing appears to be happening. If the irradiance is terminated during this time, no significant decomposition of the exposed surface is observed. Figure 26a shows a sample of nitramine propellant subjected to an irradiance of 836 J/cm^2 s for a period of time just prior to "first gasification" as evidenced by "first light" detected by the photodiode. It is not until the first gasification time is achieved that the sample starts to significantly decompose. The irradiance has established and deepened the thermal profile in the

solid until a surface temperature is reached that causes significant ablation/ decomposition at the surface. For exposures slightly longer than the time necesary for this initial gasification, the sample continues to gasify but does not ignite in the classic sense of ignition. That is, if the irradiance is removed, the sample will cease gasifying, the temperature profile in the solid will collapse, and the sample will not combust. Figure 26b shows a sample subjected to 836 J/cm^2 s at a time just after first gasification (as evidenced by first light) which displays some decomposition at the surface. Figure 26c shows another sample under the same conditions at a time just less than that required for go/no-go ignition. Although this sample shows significant decomposition, ignition will not take place until the condition of irradiance-time associated with the curve "go/no-go ignition" in Figure 25 has been achieved. At this time, and for longer exposure times, the sample is ignited, i.e. if the external irradiance is removed the sample will continue to burn [104].

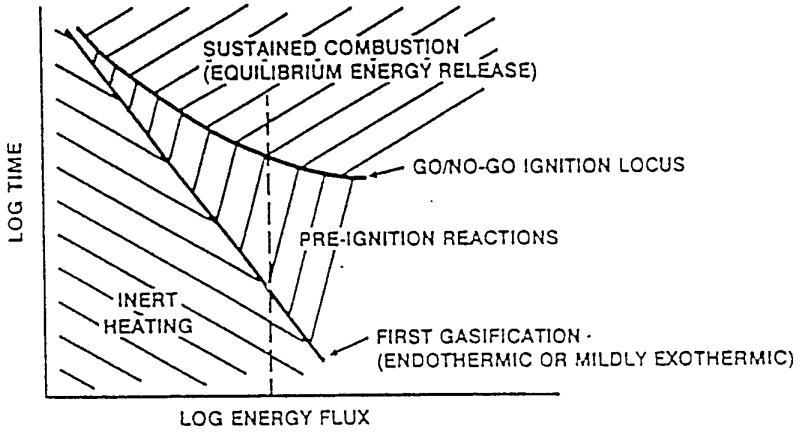

Figure 25: Generalised ignition map [102].

There exists another region called "overdriven combustion" associated with higher irradiance and steeper thermal profile [105] where removal of the irradiance will cause the sample to extinguish. Some caution, however, must be exercised. Propellant ignition should not be simply viewed as a switch based on a critical temperature associated with the surface temperature of the solid; that is, if these conditions are satisfied, an instantaneous change is made from a non-reacting solid to one burning at steady state yielding fully reacted gases. The pre-ignition region is important in that in this region the solid has decomposed into reactive intermediate species, i.e. pyrolysis products, but these species have not reacted to final products, therefore self-sustained combustion has not been achieved. Composite AP propellants tested at low irradiance levels and high pressures may show little or no detectable differences between go/no-go and first gasification. On the other hand, nitramine-based propellants under similar conditions displayed significant pre-ignition behaviour. Pre-ignition behaviour can be

demonstrated in AP-based propellants by increasing the irradiance and decreasing the test pressure [106]. It has been cautioned against using light emission, even in the infrared, as a criterion for ignition because there was no correlation between increased pressures and luminosity readings during the laser heating time [107]. The burning and glowing of graphite particles used as coating materials for the propellant grains were found to cause the occurrence of luminous zones before any pressure increase was observed. For this reason, a reliable ignition event for the single base propellant BTU85 was considered to occur only when a pressure of 10 MPa was attained [107].

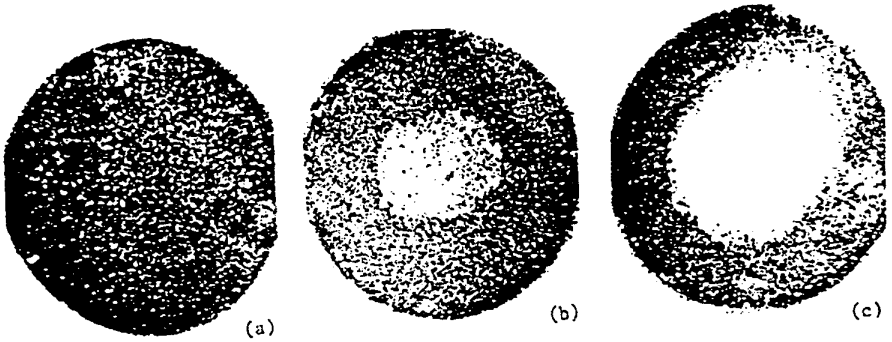

Figure 26: A sample of nitramine-based propellant exposed to 836 J/cm² s laser irradiance at a time (a) prior to first light/gasification, (b) after first light/gasification, and (c) preceding go/no-go or complete ignition [103].

4.3.4 Instrumentation

By far the greatest amount of recent work in solid propellant ignition has utilized radiant energy as stimulus for ignition. Hermance [81] has discussed the advantages and drawbacks associated with the earlier use of shock tubes, igniters, hot plates and muffle furnaces. Ohlemiller and Summerfield [100], and Fishman and Bayer [108], have evaluated the merits of earlier radiative ignition studies. The spectral range of energy sources (not to scale) and the IR detector response is shown in Figure 27. Note that the CO_2 laser and the xenon arc are at opposite ends of the wavelength scale and the laser is monochromatic whereas the arc is panchromatic.

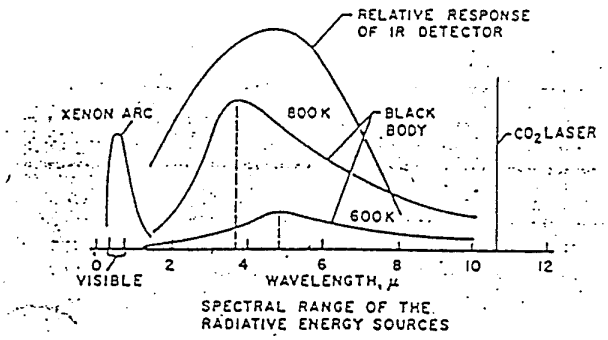

Figure 27: Spectral range of energy source and IR detector response.

Atwood et al. [103] described the ignition facilities at the Naval Weapons Center (NWC) which consist of two radiant energy sources: a xenon arc image and a CO_2 laser. A schematic diagram of the CO_2 laser ignition system at NWC is shown in Figure 28. The system consists of the energy source, external electronics and ignition apparatus. The energy source is the CO_2 laser output at 450 watts at 10.6 μm. The external electronics provide pulse control and record test data. The ignition apparatus contains the combustion chamber with sample holder, lens system and chopper wheel. Laser light passes through a long focal length lens system to decrease the overall beam diameter. The chopper located at the focal point of the lens system provides a square energy pulse. The laser enters the combustion chamber through a ZnSe window and strikes the propellant sample. First light/gasification is detected by a light sensing photodiode. Output from the oscilloscope includes the duration of the laser pulse, the photodiode first light, and calorimeter output. Electronically gated pulsing coupled with an external chopper wheel rotation controls the sample exposure time. The minium irradiance from this system is 105 W/cm^2, while the maximum is 836 W/cm^2. Coating of the sample with ZrC is necessary to provide more uniform absorptivity at the propellant surface [103] although graphite coating materials were known to give rise to non-ignition related luminosity readings [107].

Neither the continuous wave CO_2 laser nor the xenon arc image produces the ideal energy input, i.e. an irradiance that is spatially uniform and totally absorbed at the propellant surface. The non-ideality effects [100,109,110] include spatial non-uniformities over the sample surface, wavelength-dependent volumetric and surface reflection, in-depth radiation absorption and scattering, and suppression of gas-phase reaction by cool ambient gas. Assessment and rationalization of the differences arising from using the two modes of radiation sources were earlier discussed by DeLuca et al. [96,101].

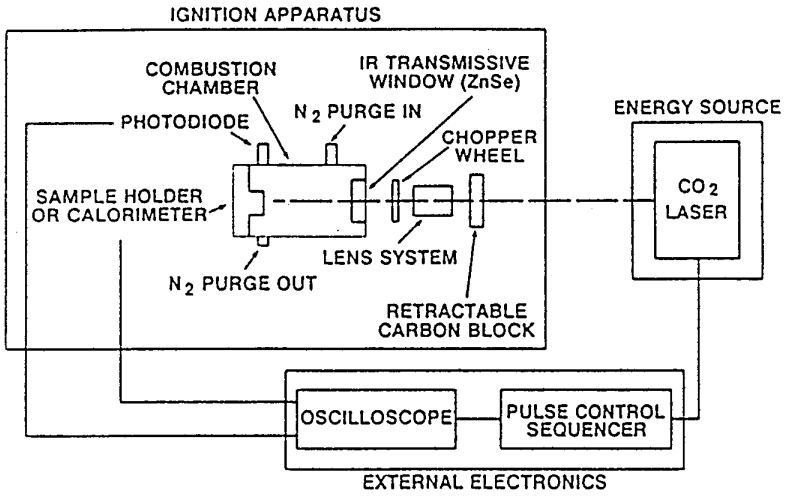

Figure 28: Schematic diagram of the CO_2 laser ignition system at the NWC [103].

Ideally, the radiant sample exposure time should be an instantaneous step function, but practically this cannot be achieved. Zurn and Atwood [111] noted the fundamental difference in rise time of the radiation from the xenon arc image and the laser CO_2 impinging upon the sample. The arc image "open" function currently averages about 3.5 ms. The rise time for the laser averages 130 μs.

A micro-motor for analysis of ignition products and an ultrasonic sensor for detection of the beginning of propellant regression were used [112]. The start of regression was noted to be very close to the beginning of ignition.

4.3.5 Propellant Systems

Hermance [81] provided an excellent review of earlier work up to 1978, mostly based on arc image studies, which includes a critical assessment of various ignition theories. More recent work using lasers was reported by DeLuca et al. [101], Lengelle et al. [112], Atwood et al. [103], and Mach [107].

Optical factors and chemical factors affect ignition delay. Optical factors can be minimized by carbon addition to opacify the propellant [96]. The combined effect of added carbon on optical properties, i.e., reflection and in-depth absorptivity, of a nitrocellulose/TMETN double base propellant yields a dramatic shift of the first light curve (i.e. L_1 boundary) to shorter times with a simultaneous increase in slope. The propellants used are summarised in Table 9 and the effect of varying carbon content was studied in detail [96].

Chemical factors influencing ignition behaviour can be inferred by examining ignition maps of different types of propellants. Since ignition boundaries are indicative of the temperature needed to initiate rapid decomposition of the propellant, the order

of ease of ignition would be expected to be the same as the order of propellant burning surface temperatures, which are, in part, a measure of the ease of the decomposition of the solids. The burning surface temperatures are as follows: double-base 260-340^{o}C [113], AP composite 700-800^{o}C [114], and HMX 1050^{o}C [115]. Thus double-base propellants are expected to ignite more easily than AP composites which in turn are more ignitable than HMX composites. However, the arc image results of De Luca et al. [101] showed no apparent trend, and this was attributed to the ignition source leading to mixed dependencies of the data on both optical properties and chemical properties.

Table 9: Propellants examined by De Luca et al. [96]

Ammonium perchlorate (AP)/hydrocarbon binder composite propellants:

Nonmetallized
1. 75% AP (45 μ) without C (batch 1086)
2. Same as 1 but with 1% C (batch 1087)
3. 80% AP (30% 15 μ and 70% 180 μ) (batch 1020)

Metallized
4. 24% AP and 51% boron

Nitrocellulose (NC) double base (DB) propellants:

5. Standard US Army M-9 (39.6% NC, 49.4% NG, 11.0% plasticizer and stabilizer)
6. Nitrocellulose (NC) Plastisol [53.7% NC, 39.2% trimethylolethane trinitrate (MTN), 7.1% triethylene glycol dinitrate (TEGDN)] (batches 1069 and 1070)
7. Opacified NC plastisol, No. 6 with 0.2% C (batch 1059)
8. Opacified NC plastisol, No. 6 with 1.0% C (batch 1088)
9. Standard US Navy N-5 (50.0% NC, 34.9% NG, 12.5% plasticizer and stabilizer, 2.6% Pb salts) (a JANNAF reference propellant)
10. Catalyzed NC plastisol, No. 6 with 2.0% lead salicylate (Pb-Sa) and copper salicylate (CuSa) and 0.2% C (batch 1050)

Nitramine (HMX)/polyurethane (PU) propellants:

11. High energy propellant 85% HMX, 15% PU)
12. Cool propellant (75% HMX, 15% PU, 10% oxamide)

An order of ignitability could be established when the optical factors were minimized by opacifying the propellant (with carbon addition) and by subtracting the reflected energy [96]. The order of increasing ease of ignitability is as follows: HMX composite < AP composite < non-catalyzed double base < catalyzed double base.

In general, the experimental results indicate that the L_{1a} limit (Figure 24) is always the basic, lowermost line for each propellant and that composite AP-based propellants are immune from the L_{1a}-L_{1d} delay. A coupling exists between the first-stage solid-phase exothermic decomposition, which takes place in a very narrow region of the solid adjacent to the surface, and the development of the final-stage gas-phase reaction. The size of the solid-phase reaction zone is governed by the transmissivity of

the solid phase and therefore the presence and importance of this stage can be magnified by ignition with radiation sources [81].

Recently, the ignition behaviour of AP-based, nitramine-based, and nitrocellulose-based propellants have been systematically examined in a study by Atwood, Price and Boggs [103]. Both xenon arc-image and CO_2 laser were employed. First light and go/no-go curves were generated as a function of irradiance (105 to 836 W/cm^2) and pressure (172.5 to 1380 kPa) (i.e. 25 to 200 psi).

The pre-ignition region diminishes as the pressure increases from 172.5 kPa to 1380 kPa (25 to 200 psi). At a common pressure and radiant exposure level, ignition time for first light and go/no-go obtained with the laser source were consistently and considerably less than the data obtained with arc image. Figure 29 shows the effect of irradiance and pressure on ignition of AP-based propellants, and Table 10 compares ignition data for arc image and laser source.

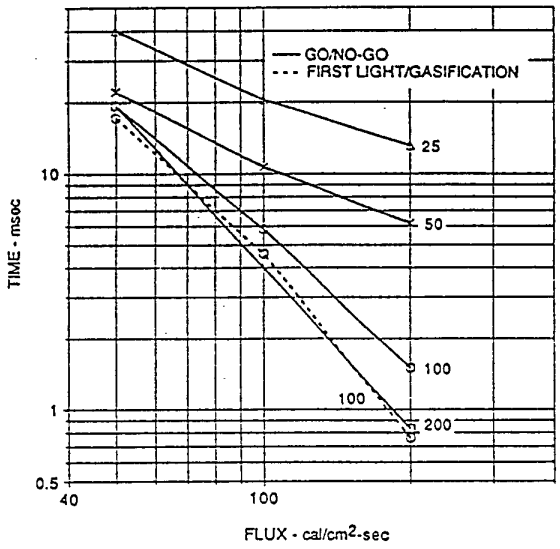

Figure 29: Effect of flux and pressure on ignition of AP-based propellants [103].

The results for non-aluminized AP composite propellants by Baer and Ryan [82,83], Inami et al. [116], DeLuca et al. [96] and of the French Office National d'Etudes et de Recherches Aerospatiales (ONERA) [112] were examined by Lengelle et al. [112]. Some conclusions emerged as follows:

(i) The nature of the radiant exposure has no influence on the time of first ignition. Only the irradiance level and its possible variation over time is important;

(ii) The degradation reaction leading to ignition is characteristic of ammonium perchlorate; and

(iii) The nature of the gases, whether inert or oxidising, has no effect on the surface temperature at ignition.

Table 10: Ignition data on AP-based propellants obtained from laser and arc image sources [103]

Method	Pressure, (psia N2)	Irradiance (cal/cm²-s)							
		25		50		100		200	
		FL*	GNG**	FL	GNG	FL	GNG	FL	GNG
Arc image	25	188.0 ± 35.0	217.5 ± 0.2	57.5 ± 2.6	56.0 ± 1.6	10.3 ± 2.7	25.5 ± 0.9		
	50	136.8 ± 27.7	190.5 ± 3.4	24.5 ± 6.4	29.8 ± 4.0	9.7 ± 2.2	15.2 ± 1.0	No AIF data at this	
	100	102.0 ± 18.6	127.3 ± 4.4	22.6 ± 3.6	33.3 ± 0.2	9.0 ± 2.4	11.0 ± 1.0	irradiance level	
	200	82.8 ± 9.2	86.1 ± 0.16	28.0 ± 4.3	26.0 ± 1.4	7.9 ± 2.0	9.0 ± 1.0		
Laser	25	No laser data at this irradiance level		25.30 ± 3.04	40.17 ± 0.22	4.92 ± 0.77	20.50 ± 1.40	1.01 ± 0.26	13.10 ± 1.33
	50			17.32 ± 3.09	22.17 ± 1.00	4.97 ± 1.13	10.67 ± 0.14	1.04 ± 0.19	6.17 ± 1.00
	100			17.16 ± 3.84	19.33 ± 1.37	4.59 ± 0.64	5.83 ± 0.22	0.76 ± 0.31	1.50 ± 0.25
	200			17.91 ± 2.57	19.33 ± 0.88	7.02 ± 1.12	8.17 ± 0.22	0.56 ± 0.16	0.83 ± 0.14

* FL = First light/gasification, in ms

** GNG = Go/no-go, in ms

Figure 30 shows the combined results examined by Lengelle et al.[112].

For highly aluminized propellants, at a given irradiance, the same ignition temperature was obtained as for un-aluminized propellants using the same AP kinetics [112]. Because the effusivity of aluminized propellants is higher, $\Gamma = 0.125$ J/Kcm^2 s$^{1/2}$, the surface temperature rises more slowly and the ignition time is longer than for non-aluminized propellants [112].

For homogeneous propellants, the start of the propellant regression rate was found to occur after the first ignition time and very close to the flame setup time [112]. Further, the exothermic reaction causing ignition occurs in the depth of the propellant, contrasting to the case of AP propellants where it takes place on the surface. The results of Thompson and Suh [117], Price et al. [109], Niioka et al. [115], and of ONERA [112] are combined in Figure 31.

Mach [107] determined the pulse energies necessary to cause a reliable ignition for single and double base propellants. The quantitative ignition criterion used was that the pressure must exceed 10 MPa. The threshold energy, i.e., the pulse energy corresponding to an ignition probability P = 0.95, was examined as a function of the free volume of the propellant bed, laser pulse power, laser beam cross-section, and propellant characteristics. The threshold energy increases with increasing chamber volume. Because large caliber ammunition requires large chamber volume, a high threshold energy is needed for ignition. The threshold energy can be minimised if the laser pulse power is minimised at constant pulse duration. The threshold energies were found to be 6.5, 4.5 and 5.0 J for the three propellants examined; BTU85, B19T98, and JA-2, respectively. The low threshold energy seems to be correlated with the high propellant explosive energy and high loading density [107].

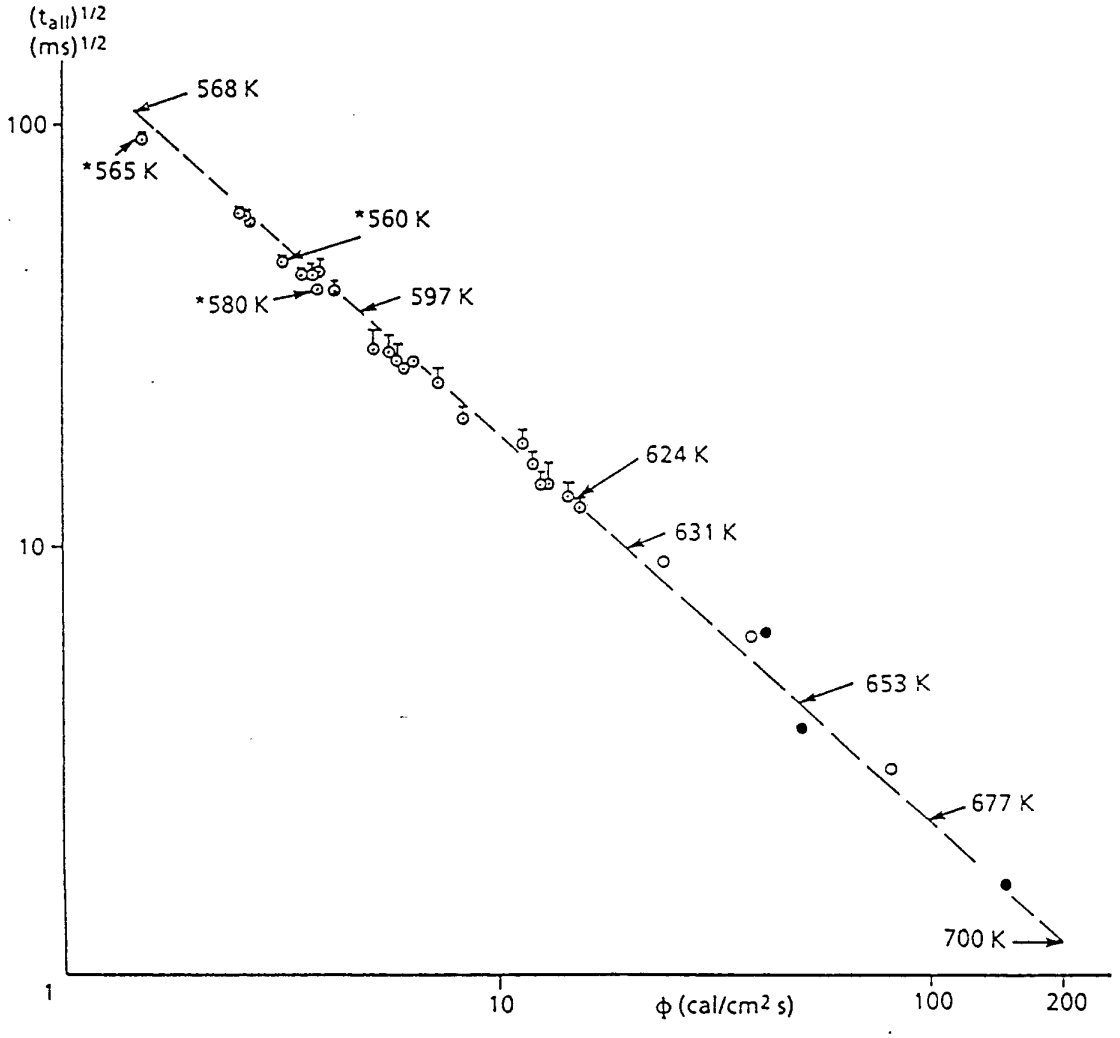

Figure 30: Combined ignition data of non-aluminized AP-propellants [112].

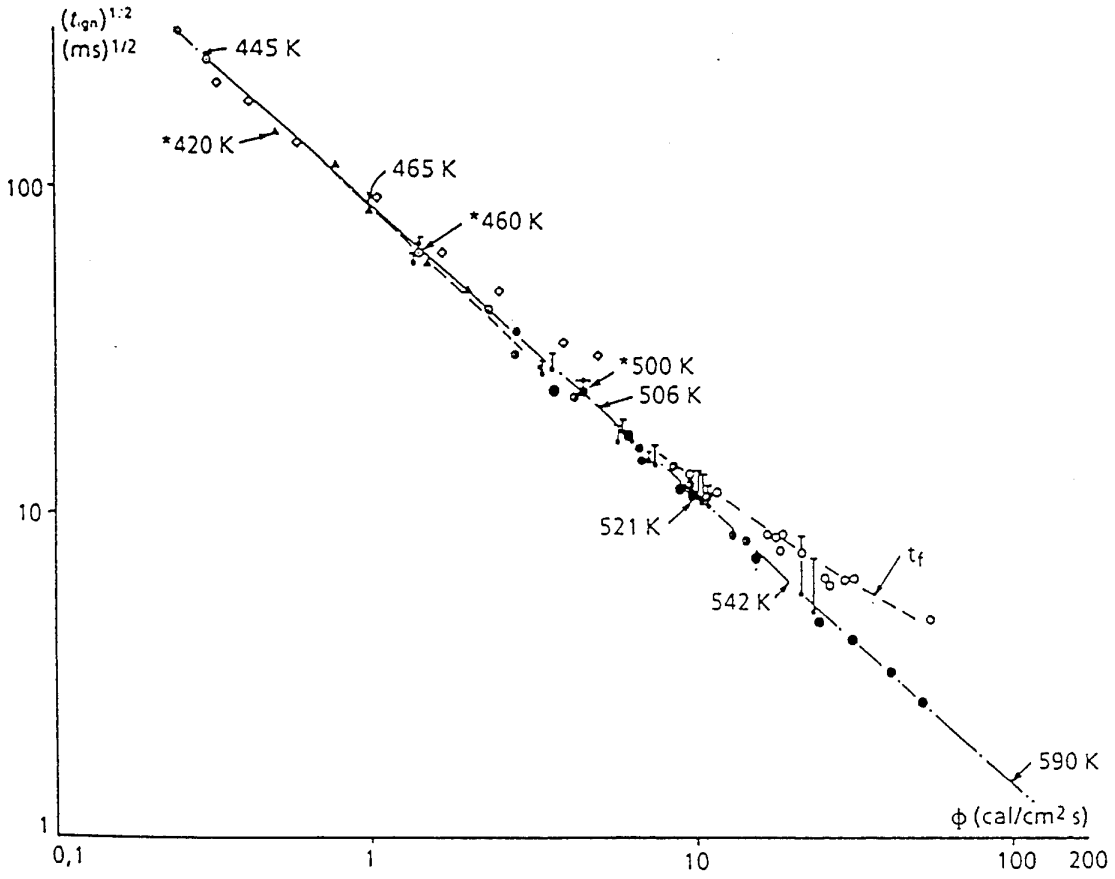

Figure 31: Combined ignition data of homogeneous propellants [112].

Figure 32 shows the effect of irradiance and pressure on a nitramine-based propellant. Table 11 compares data for arc image and laser source. In contrast to the pressure-dependent first light times for the AP-based propellants, first light times for the nitramine-based propellants are relatively independent of pressure. On the other hand, go/no-go time for the nitramine-based propellant is strongly dependent on pressure, decreasing considerably by up to a factor of 7 when pressure increased from 1035 to 1725 kPa (i.e. 150 to 250 psi). Ignition times for first light and go/no-go obtained with a laser source for nitramine-based propellants, in common with AP propellants, are consistently less than data obtained with arc image. The faster ignition process taking place in the laser was attributed to absorption of energy in the gas phase [102].

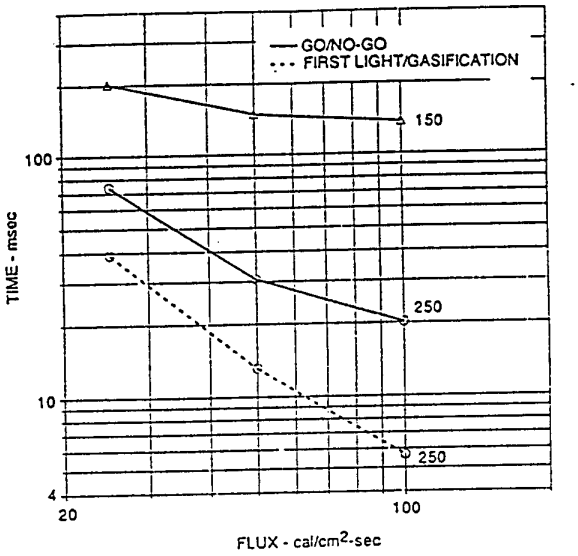

Figure 32: Effect of flux and pressure on nitramine-based propellants [103].

Table 11: Ignition data on nitramine-based propellants obtained from laser and arc image sources [103]

Method	Pressure, (psia N2)	Irradiance (cal/cm²-s)							
		25		50		100		200	
		FL*	GNG**	FL	GNG	FL	GNG	FL	GNG
Arc image	150	44.50 ± 9.50	202.00 ± 5.20	13.00 ± 2.80	148.50 ± 6.00	5.20 ± 0.80	136.70 ± 4.40	No AF data at this irradiance level	
	250	39.74 ± 5.20	70.00 ± 0.25	18.44 ± 1.70	30.64 ± 0.69	5.66 ± 0.70	20.21 ± 1.90		
Laser	150	No laser data at this irradiance level		11.20 ± 1.50	53.67 ± 0.22	3.57 ± 0.36	77.86 ± 2.44	1.50 ± 0.11	70.33 ± 2.50
	250			10.58 ±1.34	17.64 ± 1.43	2.69 ± 0.18	11.36 ± 0.69	0.91 ± 0.02	11.50 ± 0.00

* FL = First light/gasification, in ms
** GNG = Go/no-go, in ms

More importantly, the effect of compositional difference reveals that while the nitramine-based propellant begins to decompose earlier than the AP-propellant, the latter achieves the critical temperature/species concentration necessary for full ignition long before the former does: see Figure 33.

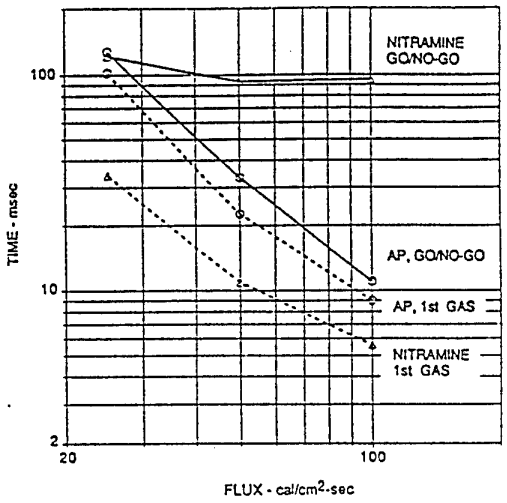

Figure 33: Comparison of ignition data on nitramine and AP propellants [103].

The effect of glycidyl azide polymer (GAP), hydroxyterminated polybutadiene (HTPB) and polycaprolactone (PC) as binder in AP-based propellants is shown in Figure 34. The GAP binder sytem is the most easy to ignite and the PC binder propellant the most difficult under these conditions [103].

Increasing the radiant exposure alone is not always sufficient to increase propellant ignitability. Ohlemiller et al. [105] demonstrated that samples may be difficult to ignite and may even be extinguished in a region of "overdriven combustion". At high radiant exposure levels, the pyrolysis products are swept away before they are able to fully react [102].

Table 12 summarises the energetic and kinetic parameters for AP, nitramine and nitrocellulose propellants determined from the analysis of ignition data [103] from these propellants. The analysis was performed according to the NWC Transient Combustion Model described by Atwood et al. [102]. Such global kinetic and energetic parameters may be applied to other evaluations of hazards including DDT and fragment impact.

Lengelle et al. [112] have established correlation equations, deduced from ignition mechanisms and corresponding kinetics, for different types of propellants such as AP composites, double-base propellants, and HMX-based propellants. In a solid propellant grain, the flow and associated flux can be evaluated by computation [118-120]. The knowledge of a characteristic ignition temperature for the propellant allows the ignition propagation along the grain to be determined [112].

Table 12: Energetic and kinetic parameters for propellant materials used in transition combustion model [103]

Model Parameters	HMX	Nitrocellulose Base Propellant	AP Based Propellant	Nitramine Based Propellant
Condensed-phase prefactor, endothermic (A_{C1})	7.09×10^{21} s^{-1}	5.65×10^{26} s^{-1}	1.44×10^{11} s^{-1}	3.71×10^{21} s^{-1}
Condensed-phase prefactor, exothermic (A_{C2})	5.92×10^{19} s^{-1}	1.63×10^{25} s^{-1}	7.14×10^{10} s^{-1}	3.64×10^{20} s^{-1}
Condensed-phase activation energy, endothermic (E_{C1})	47.8 kcal/mol	49.0 kcal/mol	27.23 kcal/mol	46.40 kcal/mol
Condensed-phase activation energy, exothermic (E_{C2})	44.3 kcal/mol	46.2 kcal/mol	26.08 kcal/mol	45.21 kcal/mol
Endothermic heat release (ΔH_1)	+ 125 cal/gm	+ 380 cal/gm	+ 414 cal/gm	+ 190 cal/gm
Exothermic heat release (ΔH_2)	- 170 cal/gm	+ 258 cal/gm	+ 279 cal/gm	- 29.2 cal/gm
Second order prefactor, gas-reaction 1 (A_{g1})	1.48×10^{11} cm^3/mol-s	1.92×10^{12} cm^3/mol-s	9.61×10^{11} cm^3/mol-s	1.68×10^{12} cm^3/mol-s
Activation energy, gas-reaction 1 (E_{g1})	19.2 kcal/mol	25.5 kcal/mol	24.05 kcal/mol	24.95 kcal/mol
Second order prefactor, gas-reaction 2 (A_{g2})	8.09×10^{14} cm^3/mol-s	1.49×10^{15} cm^3/mol-s	4.29×10^{14} cm^3/mol-s	3.88×10^{14} cm^3/mol-s
Activation energy, gas-reaction 2 (E_{g2})	25.6 kcal/mol	23.5 kcal/mol	23.5 kcal/mol	26.14 kcal/mol
Thermal conductivity, condensed-phase (λ_s)	0.001295 cal/cm-s-deg	0.000470 cal/cm-s-deg	0.001034 cal/cm-s-deg	0.000880 cal/cm-s-deg
Thermal conductivity, gas-phase (λ_g)	0.000800 cal/cm-s-deg	0.000800 cal/cm-s-deg	0.000800 cal/cm-s-deg	0.000800 cal/cm-s-deg
Specific heat, condensed-phase (C_{ps})	-0.28 cal/gm-deg	0.38 cal/gm-deg	-0.32 cal/gm-deg	-0.32 cal/gm-deg
Specific heat, gas-phase (C_{pg})	0.43 cal/gm-deg	0.43 cal/gm-deg	0.42 cal/gm-deg	0.41 cal/gm-deg
Density, condensed-phase (ρ_s)	1.912 gm/cm^3	1.581 gm/cm^3	1.779 gm/cm^3	1.859 gm/cm^3
Overall reaction heat release (ΔH_r)	1314 cal/gm	943 cal/gm	920 cal/gm	962 cal/gm
Phase transition temperature (T_{tr})	521 K	-	513 K	521 K
Heat of transition (ΔH_{tr})	845 cal/gm	-	14.0 cal/gm	3.4 cal/gm
Melting temperature (Tm)	-	-	862 K	-
Heat of melting (ΔH_m)	-	-	41 cal/gm	-

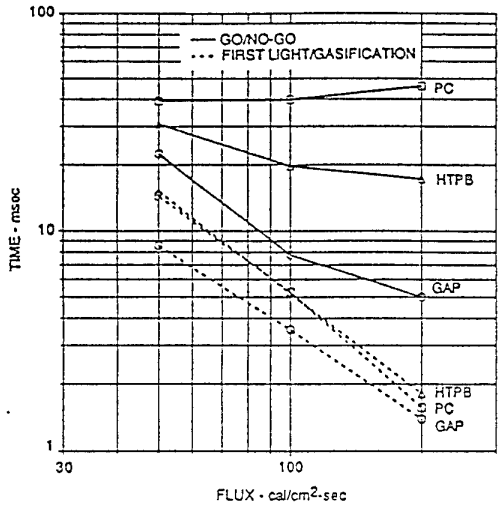

Figure 34: Effect of various binders on ignition data of AP-based propellants [103].

4.3.6 Summary

Weapon systems incorporating direct laser ignition of solid propellants are still under active R&D overseas. For large-caliber guns, direct laser-induced ignition of propellants is only feasible if multipoint ignition is used, or if laser ignition of a pyrotechnic primer is employed to substantially ignite the propellant.

From a practical point of view, the assessment and ranking of propellant ignitability using a controller laser source is useful for evaluation of the hazard potential with respect to planned or accidental stimuli. This basic research can ultimately identify propellants meeting the requirements for insensitive munition developments.

The position and ignition behaviour boundaries of a given propellant can be rationalized in terms of the reactivity of the energetic materials and the efficiency with which the incident radiant heat is utilised. In comparative ignitability ranking, the latter factor can obscure the underlying propellant reactivity effects. When the inefficient use of incident energy is removed by opacifying the propellant and subtracting the reflected energy, the true underlying chemical effect can be evaluated [96,101].

Hermance [81] is of the contention that perhaps we still do not know if there is one and only one dominant mechanism for solid propellant ignition. A purely solid phase reaction mechanism is not the dominant mechanism of ignition in either double base or composite propellants, and the weight of theoretical evidence appears to favour

phase reaction processes over heterogeneous reaction processes as being dominant in shock tube and radiant ignition situations.

There is good experimental [96,101,105,121] and theoretical [115,122, 123] evidence that the notion to regard the start of ignition as a runaway at some temperature after raising from an initial low value is not always valid. Hermance [81] pointed out that a material is not really ignited until it finally burns steadily. Further experimental and theoretical investigations on transition to steady-state burning is required to resolve these issues. The application of Coherent Anti-Stoke Raman Spectroscopy (CARS) to monitor chemical species development and of Laser Doppler Velocimetry to monitor surface regression rate instead of the use of light emission photodiode technology may prove useful to understand the various transition stages which lead to achievement of steady-state burning.

5. Conclusion

Laser initiated weapon subsystems have numerous advantages compared to conventional bridgewire initiators. The principle ones are their immunity from electromagnetic fields, electrostatic discharge or stray electrical energy, the potential for use of less sensitive explosives or pyrotechnics in the initiator due to the greater power output of the laser, built-in self test without affecting safety and the potential for less complex and wholly electronic safety and arming systems providing fast acting and precise timing.

Many examples exist of the use of laser initiators in weapon subsystems under development. These include the Space Shuttle Advanced Solid Rocket Motor, Laser Initiated Caseless Ammunition, egress systems for the B-1B, F-16 and the JPATS, Explosive Ordnance Disposal systems, the Advanced Air to Air Missile and the US Ground Based Interceptor Program. However, the authors are not aware of any laser ordnance initiation systems that have been fully qualified and fielded in a practical weapon system.

The current state of technology of laser initiation of explosives, pyrotechnics and propellants has been evaluated.

For explosives, the three major methods of initiation (direct laser initiation, a thin film in contact with the explosive, and flyer plate launch and impact) have been discussed and evaluated. The effect of the explosive physical variables and igniter hardware design on the threshold ignition energies have been examined. The use of direct laser intiation as a tool to probe the decomposition process of explosives was also noted. It has been concluded that the only possible approach to laser initiation of explosives in a fuze is via laser driven flyer plates. Currently the cost and size of prototypes are too great for incorporation in most practical systems.

An extensive examination of the range of pyrotechnic compositions that have been initiated by different lasers has been undertaken. The effect of the composition physical and chemical variables as well as the laser and igniter hardware design on the time to ignition and ignition energy and power thresholds have been discussed. The current state of research on modelling laser ignition and the difference between modelling and experiment has been presented. Based on details of current practical laser igniter designs and their performance, it would appear that this technology has reached a significant degree of maturity and laser initiated pyrotechnic igniters are likely to be qualified for service use in the near future.

Past and current work dealing with the ignition response of solid propellants to the CO_2 laser as a radiative source is outlined and, where appropriate, comparison is made between the results obtained with the laser source and those with the xenon arc image furnace. The effects of changes in propellant formulations and of various types of propellants on the ease of ignitability are discussed. The principal ignition theories of solid propellants are summarised, and a detailed description of the sequence of events taking place during an ignition process is given in the ignition map. For propellants, the principal applications of ignition data are in the assessment of the overall hazard potential with respect to planned or accidental ignition stimuli and in the determination of global energetic and kinetic parameters.

Laser initiation is an advanced technology which will emerge in the initiation trains of weapon subsystems in the near future. Their application will almost exclusively be driven by safety requirements and cost constraints and will be focussed on the ignition of pyrotechnics and explosives.

6. References

1. Zimmerman, C.J., and Litzinger, G.E. (1993).
Introduction of Laser Initiation for the 48-inch Advanced Solid Rocket Motor (ASRM) at Marshall Space Flight Centre, The First NASA Aerospace Pyrotechnic Systems Workshop, NASA Stennis Space Centre, pp. 157-177.

2. Yang, L.C. and Menichelli, V.J. (1976).
Laser initiation of insensitive high explosives. Proc. 6th Symposium (Int.) on Detonation. p 612.

3. Tasaki, Y., Kurokawa, K., Hattori K., Sato,T., Miyajima, T. and Takano, M. (1982).
Experimental study of laser initiated detonator. 4th Congres International de Pyrotechnics, La Grande Motie, France.

4. Bykhalo, A.I., Zhuzhukalo, E.V., Koval'skii, N.G., Kolomiitskii, A.N., Korobov, V.V., Rozhkov, A.D. and Yudin, A.I. (1986).
Initiation of PETN by high-power laser radiation. *Combustion, Explosives and Shockwaves,* p 481. Plenum.

5. Paisley, D.L. (1989).
Prompt detonation of secondary explosives by laser. Proc. 9th Symposium (Int.) on Detonation. p 1110.

6. Renlund, A.M., Stanton, P.L. and Trott, W.M. (1989).
Laser initiation of secondary explosives. Proc. 9th Symposium (Int.) on Detonation. p 1118.

7. Sheffield, S.A., Rogers Jr., J.W. and Castaneda, J.N. (1985).
Velocity measurements of laser-driven flyer plates backed by high impedance windows. *APS Shock Waves in Condensed Matter.* Gupta, Y.M. (ed.). Plenum.

8. Paisley, D.L. (1990).
Laser-driven miniature flyer plates for shock initiation of secondary explosives. *Shock Compression of Condensed Matter.* Schmidt, S.C., Johnson, J.N., and Davison, L.W. (eds.). Elsevier.

9. Dobratz, B.M. (1981).
LLNL Explosives handbook. *Properties of chemical explosives and explosive simulants.* UCRL-52997.

10. Weingart, R.C., Lee, R.S., Jackson, R.K., and Parker, N.L. (1976).
Acceleration of thin flyer plates by exploding metal foils: Application to initiation studies. Proc. 6th Symposium (Int.) on Detonation. p 653.

11. Ostmark, H. (1992).
Laser ignition of explosives: A parametric and spectroscopic study. TRITA-FYK 9201, Stockholm, Sweden.

12. Ng, W.L., Field, J.E., and Hauser, H.M. (1986).
Thermal, fracture, and laser-induced decomposition of pentaerythritol tetranitrate. *J. Appl. Phys.* 59, 3945.

13. Tang, T.B., Chaudhri, M.M., Rees, C.S., and Mullock, S.J. (1987).
Decomposition of solid explosives by laser irradiation: a mass spectrometric study. *J. Materials Science* 22, 1037.

14. Sheffield, S.A. and Fisk, G.A. (1983).
Particle velocity measurements in laser irradiated foils using ORVIS. *APS Shock Waves in Condensed Matter.* Asay, J.R., Graham, R.A., and Straub, G.K. (eds.). Elsevier.

15. King, T., Barrus, D., Dingus, R., Osborne, Z. and Phipps, C. (1986). *Measurements of laser generated impulse.* Proceedings of the International Symposium on Intense Dynamic Loading and its Effects, Beijing, China.

16. Ripin, B.H., Decoste, A., Obenschain, S.P., Bodner, S.E., McLean, E.A., Young, F.C., Whitlock, R.R., Armstrong, C.M., Grun, J., Stamper, J.A., Gold, S.H., Nagel, D.J., Lehmberg, R.H., and McMahon, J.M. (1980). Laser-plasma interaction and ablative acceleration of thin foils at 10^{12}-10^{15} W/cm^2. *Phys. Fluids,* 23, 1012.

17. Obenschain, S.P., Whitlock, R.R., McLean, E.A., Ripin, B.H., Price, R.H., Phillion, D.W., Campbell, E.M., Rosen, M.D., and Auerbach, J.M. (1983). Uniform ablative acceleration of targets by laser irradiation at 10^{14} W/cm^2. *Physical Rev. Letts.*, 50, 44.

18. Mayer, F.J. and Busch, G. E. (1985). Plasma production by laser-driven explosively heated thin metal films. *J. Appl. Phys.*, 57, 827.

19. Fairand, B.P. and Clauer, A.H. (1979). Laser generation of high-amplitude stress waves in materials. *J. Appl. Phys.* 50, 1497.

20. Cottet, F. and Boustie, M. (1989). Spallation studies in aluminum targets using shock waves induced by laser irradiation at various pulse durations. *J. Appl. Phys.* 66, 4067.

21. Ballard, P., Fournier, J., Fabbro, R., Frelat, J., Castex, L. (1989). Residual stresses induced by laser shocks. *Shock compression of condensed matter,* Schmidt, S.C., Johnson, J.N., and Davison, L.W. (eds). Elsevier.

22. Eliezer, S., Gazit, Y., and Gilath, I. (1990). Shock wave decay and spall strength in laser-matter interaction. *J. Appl. Phys.* 68, 356.

23. Paisely, D.L. (1992). Laser-driven miniature plates for one-dimensional impacts at 0.5 -≥ 6 km/s. *Shock-wave and high-strain-rate phenomena in materials.* Meyers, M.A., Murr, L.E., and Staudhammer, K.P. (eds). Marcel Dekker.

24. Walters, C.T. (1991). Laser generation of 100-kbar shock waves in solids. *Shock compression of condensed matter,* Schmidt, S.C., Dick, R.D., Forbes, J.W., and Tasker, D.G. (eds) Elsevier.

25. Krehl, P., Schwirke, F., and Cooper, A.W. (1975). Plasma produced by laser irradiation of plane solid targets. *J. Appl. Phys.* 46, 4400.

26. Chen, F.F. (1977).
Introduction to plasma physics. Plenum.

27. Griffin, R.D., Justus, B.L., Campillo, A.J., and Goldberg, L.S. (1986).
Interferometric studies of the pressure of a confined laser-heated plasma.
J. Appl. Phys. 59, 1968.

28. Cottet, F., Marty, L., Hallouin, M., Romain, J.P., Virmont, J., Fabbro, R., and Faral, B. (1988).
Two-dimensional study of shock breakout at the rear face of laser irradiated metallic targets. *J. Appl. Phys.* 64, 4474.

29. Trott, W.M. (1991)
Studies of laser-driven flyer acceleration using optical fiber coupling. *Shock compression of condensed matter*, Schmidt, S.C., Dick, R.D., Forbes, J.W., and Tasker, D.G. (eds) Elsevier.

30. Romain, J.P. and Zagouri, D. (1991).
Laser-shock studies using an electromagnetic gauge for particle velocity measurements. *Shock compression of condensed matter.* Schmidt, S.C., Dick, R.D., Forbes, J.W., and Tasker, D.G. (eds). Elsevier.

31. Trott, W.M. and Meeks, K.D. (1989).
Acceleration of thin foil targets using fiber-coupled optical pulses. *Shock compression of condensed matter.* Schmidt, S.C., Johnson, J.N., and Davison, L.W. (eds). Elsevier.

32. Farnsworth, A.V. and Lawrence, R.J. (1991).
Numerical and analytical analysis of thin laser-driven flyer plates.
Shock compression of condensed matter. Schmidt, S.C., Dick, R.D., Forbes, J.W., and Tasker, D.G. (eds). Elsevier.

33. Paisley, D.L., Montoya, N.I., Stahl, D.B. and Garcia, I.A. (1989).
Interferometry and high speed photography of laser driven flyer plates. *SPIE Ultrahigh Speed and High Speed Photography, Photonics, and Videography.*

34. Paisley, D.L., Warnes, R.H., and Koop, R.A. (1991).
Laser-driven flat plate impacts to 100 GPa with sub-nanosecond pulse duration and resolution for material property studies. LA-UR-91-3306.

35. Schwarz, A.C. (1981).
Shock initiation sensitivity of Hexanitrostilbene (HNS). Proc. 7th Symposium (Int.) on Detonation. p 1024.

36. Barker, L.M. and Hollenbach, A.E. (1965).
Interferometer technique of measuring dynamic mechanical properties of materials. *Rev. Sci. Inst.* 36, 1617.

37. Paisley, D.L., Montoya, N.I., Stahl, D.B., Garcia, I.A. and Hemsing, W.F. (1990).
Velocity interferometry of miniature flyer plates with sub-nanosecond time resolution. SPIE High Speed Conference, San Diego, USA.

38. Bloomquist, D.D. and Sheffield, S.A. (1983).
Optically recording interferometer for velocity measurements with subnanosecond resolution. *J. Appl. Phys.* 54, 1717.

39. Menichelli, V.J. and Yang, L.C. (1970).
Sensitivity of Explosives to Laser Energy, NASA, Technical Report 32-1474, Jet Propulsion Laboratory, California Institute of Technology, Pasadena, CA.

40. Brish, A.A., Galeev, A., Zaitsev, B.N., Sbitnev,E.A., and Tatarintsev,L.V. (1966).
Fizika Goreniya i Vzryva, 2,1 32.

41. Brish, A.A, Galeev,A., Zaitsev,B.N., Sbitnev,E.A., and Tatarintsev,L.V. (1969).
Fizika Goreniya i Vzryva, 5, 475 (1969).

42. Holst,G. (1979).
J. Ballistics, 3, 4, 627.

43. Oestmark, H. (1985).
Laser as a Tool in the Sensitivity Testing of Explosives, Proceedings of the 8th Symposium (International) on Detonation, Albuquerque, NM.

44. Oestmark, H. (1987).
Laser Ignition of Explosives: Ignition Energy Dependence of Particle Size, Proceedings of the 12th International Pyrotechnics Seminar, Juan-les Pins, France.

45. Oestmark,H. and Roman, N. (1993).
Laser Ignition of Explosives: Pyrotechnic Ignition Mechanisms, *J. Appl. Phys.*, 73 (4), 1993-2003.

46. Chow, C.T., Mohler, J.A. and Abney, L.D. (1985).
Ignition Study of Thermite Using a Laser, Proceedings of the DARPA/ARMY Symposium on Self- Propagating High Temperature Synthesis, Florida, USA.

47. Chow, C. and Mohler, J. (1987).
Thermal Ignition of Pyrotechnics With Lasers, Proceedings of the 12th International Pyrotechnics Seminar,Juan-les-Pins, France.

48. Holy, J. (1986).
Laser Ignition of $TiH_x/KClO_4$, Proceedings of the 11th International Pyrotechnics Seminar, Vail, CO. USA. 1986

49. Jungst, R. and Salas, F. (1990).
Diode Laser Ignition of Explosives and Pyrotechnic Components,
OE 90 Symposium.

50. de Yong, L. and Valenta, F. (1990).
A Study of the Radiant Ignition of a Range of Pyrotechnic Materials Using a CO_2 Laser, MRL-TR-90-20, Materials Research Laboratory, Australia.

51. Kunz, S. and Salas,F. (1988).
Diode Laser Ignition of High Explosives and Pyrotechnics, Proceedings of the 13th International Pyrotechnics Seminar, Grand Junction, CO, USA.

52. Holy, J. and Girman, T. (1988).
The Effects of Pressure on Laser Initiation of $TiH_x/KClO_4$ and Other Pyrotechnics, Proceedings of the 13th International Pyrotechnics Seminar, Grand Junction, CO,USA, 1988.

53. Ewick, D. and Beckman, T. (1990).
Ignition Testing of Low Energy Laser Diode Ignited Components, Mound Technologies, MLM-MU-90-64-003, Miamisberg, OH, USA.

54. Ewick, D. Dosser, L., McComb, S. and Brodsky, L. (1988).
Feasability of a Laser Ignited Pyrotechnic Device, Proceedings of the 13th International Pyrotechnics Seminar, Grand Junction, CO, USA.

55. Rontey, D. and Petrick, J. (1988).
Laser Ignition of $Zr/KClO_4$ Pyrotechnic Mixtures, Proceedings of the American Defence Preparedness Association Annual Meeting - Pyrotechnics Section, Shreveport, LA.

56. Fetheroff, B., Sneyder, T. , Bates, M., Peretz, A. and Kuo, K. (1989).
Combustion Characteristics and CO_2 Laser Ignition Behaviour of Boron/Magnesium/PTFE Pyrotechnics, Proceedings of the 14th International Pyrotechnics Seminar, Jersey, UK.

57. Ramadhan, F.A., Haq, I.U. and Chaudhri, M.M. (1993).
Low Energy Laser Initiation of Magnesium-Teflon-Viton Compositions,
J. Phys D: Appl. Phys., 26, 880-887.

58. Brochier, M. (1988).
A Contribution to the Study of Laser Based Ignition of Pyrotechnic Substances,
Proceedings of the 19th ICT Conference.

59. Fetheroff, B., Liiva, P., Hsieh, W. and Kuo, K. (1991).
CO_2 Laser Ignition Behaviour of Several Pyrotechnic Mixtures, Proceedings of the 16th International Pyrotechnics Seminar, Jonkoping, Sweden.

60. Kordel, E. (1990).
Laser - A Potential Candidate for Insensitive Ignition Systems, Proceedings of the Insensitive Munitions Technology Symposium, American Defence Preparedness Association, Naval Surface Warfare Centre, White Oak, Maryland, USA.

61. Refouvelet, J. and Baldy, P. (1987).
Initiation of Cartridge Igniters by Laser Radiation, Proceedings of the 12th International Pyrotechnics Seminar, Juan-les-Pins, France.

62. Ewick, D. (1990).
Finite Difference Modelling of Laser Diode Ignited Components, Proceedings of the 15th International Pyrotechnics Seminar, Boulder, CO, USA.

63. Skocypec, R. (1990).
Modelling Laser ignition of Explosives and Pyrotechnics: Effects and Characterisation of Radiative Transfer, Proceedings of the 15th International Pyrotechnics Seminar, Boulder, CO, USA.

64. Ewick, D. (1992).
Improved 2-D Finite Difference Model for Laser Diode Ignited Components, Proceedings of the 18th International pyrotechnics Seminar, Breckenridge, CO. USA

65. Glass, M., Merson, J. and Salas, F. (1992).
Modelling Low Energy Laser Ignition of Explosives and Pyrotechnic Powders, Proceedings of the 18th International Pyrotechnics Seminar, Breckenridge, CO, USA.

66. Kaminskii ,A., Bodrestova, A. and Levikor, S. (1969).
Pyrotechnically Excited Quasi-CW Laser, *Soviet Physics - Technical Physics*, 14, No 3.

67. Yang, L.C. and Cook, J.R. (1984).
Optically Pumped Neodymium Glass Laser Using Chemical Flashbulbs, IHTR-851, Naval Ordnance Station, Indian Head, Maryland, USA.

68. Jungst, R., Salas, F., Watkins, R. and Kovucic, L. (1990).
Development of Diode Laser Ignited Pyrotechnic and Explosive Components, Proceedings of the 15th International Pyrotechnics Seminar, Boulder, CO. USA.

69. Petrick, J. (1988).
Laser Ignition Systems for Pyrotechnic Applications, Proceedings of the American Defence Preparedness Association Annual Meeting - Pyrotechnics Section, Shreveport, LA. USA.

70. Landry, M. (1991).
Laser Used as Optical Source for Initiating Explosives, Proceedings of the 16th International Pyrotechnics Seminar, Jönkoping, Sweden.

71. Landry, M. and Cobbett, J. (1991).
Laser Ordnance Initiation System (LOIS) for Aircrew Egress Systems, Proceedings of the 16th International Pyrotechnics Seminar, Jönkoping, Sweden.

72. Blachowski, T. (1992).
Advanced Development of the Laser Initiated Transfer Energy Subsystem (LITES), Proceedings of the 18th International Pyrotechnics Seminar, Breckenridge, CO,USA.

73. Kramer, D. , Spangler, E. and Beckman, T. (1993).
Laser Ignited Explosive and Pyrotechnic Components, *American Ceramic Society Bulletin*, 22, 2, 78.

74. Rupert, N., Frank, K. and Moore, C. (1992).
Development of a Laser Ignition System for a Laboratory 120 mm Gun, Proceedings of the 13th Symposium on Ballistics, Stockholm, Sweden.

75. Chow, C. and Mohler, J. (1987).
Thermal Ignition of Pyrotechnics with Lasers, Proceedings of the 12th International Pyrotechnics Seminar, Juan-les-Pins, France.

76. Hicks, B.L. (1954).
Theory of Ignition Considered as Thermal Reaction, *J. Chemical Physics*, 22, pp. 414-429 (1954).

77. Price, E.W., Bradley, H.H., Dehority, G.L., and Ibiricu, M.M. (1966).
Theory of Ignition of Solid Propellants, *AIAA J.*, pp. 1153-1181.

78. Brown, R.S., Anderson, R., and Shannon, L.J. (1968).
Ignition and Combustion of Solid Rocket Propellants, *Advanced Chemical Engineering*, Vol 7, Academic Press, New York, pp-1-68.

79. Kulkarni, A.K., Kumar, M., and Kuo, K.K. (1980).
Review of Solid Propellants Ignition Studies, AIAA Paper 80-120.

80. Kishore, K. and Gayathri, V. (1984).
Chemistry of Ignition and Combustion of Ammonium-Perchlorate-Based Propellants, Chapter 2, in Series Progress in Astronautics and Aeronautics: Vol 90, Fundamentals of Solid Propellant Combustion, Edt. K. Kuo and M. Summerfield, AIAA, pp. 53-119.

81. Hermance, C.E. (1984).
Solid Propellants Ignition Theories and Experiments, Chapter 5, in Series Progress in Astronautics and Aeronautics: Vol 90, Fundamentals of Solid Propellant Combustion, Edt. K. Kuo and M. Summerfield, AIAA, pp. 239-304.

82. Baer, A.D. and Ryan, N.W. (1965).
Ignition of Composite Propellants by Low Radiance Flux, *AIAA J.*, Vol 3 (5), pp. 884-889.

83. Baer, S.D. and Ryan, N.W. (1968).
An Approximate but Complete Model for the Ignition Response of Solid Propellants, *AIAA J.*, 6, pp. 872-877.

84. Bradley, H.H. (1970).
Theory of Ignition of a Reactive Solid by Constant Energy Flux, *Combustion Science and Technology*, 2, pp. 11-20.

85. (a) Linan, A. and Crespo, A. (1972).
An Asymptotic Analysis of Radiant and Hypergolic Heterogeneous Ignition of Solid Propellants, *Combustion Science and Technology*, 6, pp. 223-23.
(b)Linan, A. and Williams, F.A. (1971).
Radiant Ignition of a Reactive Solid by Constant Energy Flux, *Combustion Science and Technology*, 3, pp. 91-98.

86. Hermance, C.E., Shinnar, R., and Summerfield, M. (1966).
Ignition of an Evaporating Fuel in a Hot Oxidising Gas, Including the Effect of Heat Feedback, *Astronautica Acta*, 12, pp. 95-112.

87. (a) Hermance, C.E., and Kumar, R.K. (1970).
Gas-Phase Ignition Theory for Homogeneous Propellants Under Shocktube Conditions, *AIAA J.*, 8, pp.1551-1558;
(b) Kumar, R.K. and Hermance, C.E., (1971).
Ignition of Solid Propellants Under Shocktube Conditions: Further Theoretical Development, *AIAA J.*, 9, 1615-1620.

88. Kumar, R.K. and Hermance, C.E. (1972).
Gas-Phase Ignition Theory of a Heterogeneous Propellant Exposed to a Hot Oxidising Gas, *Combustion Science Technology*, 4, pp. 191-196.

89. Shannon, L.J. and Deverall, L.I. (1969).
A Model of Solid Propellant Ignition in a Neutral Environment, *AIAA J*, 7, pp. 497-502.

90. Kumar, R.K. and Hermance, C.E. (1976).
Role of Gas-Phase Reactions During Radiation Ignition of Solid Propellants, *Combustion Science and Technology*, 14, 169-175.

91. Kashiwagi, T. (1974).
A Radiative Ignition Model of a Solid Fuel, *Combustion Science and Technology*, 8, pp. 225-236.

92. Kindelan, M. and Williams, F.A. (1975).
(a) Theory of Endothermic Gasification of a Solid by Constant Energy Flux, *Combustion Science and Technology*, 10, pp. 1-19;
(b) Radiant Ignition of a Combustible Solid with Gas-Phase Exothermicity, *Acta Astronautica.*, 2, (1975), pp. 955-979;
(c) Gas-Phase Ignition of a Solid Propellant with In-Depth Absorption of Radiation, *Combustion Science and Technolgy*, 16, (1977), pp. 47-58.

93. Bradley, H.H. and Williams, F.A. (1970).
Theory of Radiant and Hypergolic Ignition of Solid Propellants, *Combustion Science and Technolgy*, 2, pp. 41-52.

94. Waldman, C.H. and Summerfield, M. (1969).
Theory of Propellant Ignition by Heterogeneous Reactions, *AIAA J.*, 7, pp. 1359-1361.

95. Linan, A. and Crespo, A. (1972).
An Asymptotic Analysis of Radiant and Hypergolic Heterogeneous Ignition of Solid Propellants, *Combustion Science and Technology*, 6, pp. 223-232.

96. De Luca, L., Caveny, L.H., Ohlemiller, T.J., and Summerfield, M. (1976).
Radiative Ignition of Solid Propellants: I. Some Formulation Effects, *AIAA J.*, Vol 14, No. 7, pp. 940-946.

97. Andersen, W.H. (1970).
Theory of Surface Ignition with Applications to Cellulose, Explosives and Propellants, *Combustion Sci. Technology*, 2, 213-221.

98. Merzhanov, A.G., and Averson, A.E. (1971).
Present State of Thermal Ignition Theory, *Combustion and Flame*, 16, pp 89-124.

99. Shannon, L.J. (1967.
Composite Propellant Ignition Mechanisms, United Technology Center, Air Force Office of Scientific Research, Arlington, Va, Final Report AFOSR 67-1765, Sept 1967.

100. Ohlemiller, T.J., and Summerfield, M. (1968).
A Critical Analysis of Arc Image Ignition of Solid Propellants, *AIAA J.*, 6, pp. 878-886.

101. De Luca L., Caveny, L.H., Ohlemiller, T.J., and Summerfield, M. (1976).
Radiative Ignition of Double Base Propellants: II. Pre-Ignition Effect and Source Effects, *AIAA J.*, 14, pp. 1111-1117.

102. Atwood, A.I., Price, C.F., Boggs, T.L., and Richter, H.P. (1988). *Transient Combustion Analysis of Energetic Materials*, ICT, pp. 1-1 to 1-7.

103. Atwood, A.I., Price, C.F., Boggs, T.L. (1991). *Ignitability Measurements of Solid Propellants*, ICT, pp. 44-1 to 44-15.

104. Boggs, T.L., Price, C.F. and Derr, R.L. (1984). *Transient Combustion: An Important Consideration in Deflagration-to-Detonation Transition*, in Proc., Advisory Group for Aerospace Research and Development (AGARD), CP-367, pp.12-1 to 12-20.

105. Ohlemiller, T.J., Caveny, L.H., DeLuca, L., and Summerfield, M. (1973). *Dynamic Effects on Ignitability Limits of Solid Propellants Subjected to Radiative Heating*, 14th Symposium (International) on Combustion, The Combustion Institute, Pittsburgh, pp. 1297-1307.

106. Crump, J.E., Atwood, A.I., Zurn, D.E. (1984). *Combustion Instability and Ignition Testing of NOS/IH Extruded Composite Propellants*, Naval Weapons Center, China Lake, CA., NWC.

107. Mach,H. (1993). *Measurement of Threshold Energies for Reliable Ignition of Solid Propellants Using a Pulsed Nd-Glass Laser*, Proceedings of the 14th International Symposium on Ballistics, Quebec, Canada.

108. Fishman, N. and Beyer, R.B. (1960). *ARS Progress in Astronautics and Rocketry: Solid Propellant Rocket Research*, Vol 1, Edt. Summerfield, M., Academic Press, p. 673.

109. Price, E.W., Bradley, H.H., Hightower, J.D., and Fleming, R.O. (1964). *Ignition of Solid Propellants*, AIAA Paper, 64-120.

110. Fleming, R.W. and Derr, R.L. (1971). *The Use of Non-Reactive Coatings in Solid Propellant Arc Image Ignition Studies*, Proceedings of the 7th JANNAF Combustion Meeting, CPIA Publ. 204, Vol 1, pp. 379-389.

111. Zurn, D.E. and Atwood, A.I. (1981). *Problems Encountered in the Installation of the NWC CO_2 Laser Ignition System*, Proc. of the 18th JANNAF Combustion Meeting, Vol III, CPIA Pub. 347, (Publication Unclassified).

112. Lengelle, G., Bizot, A., Duterque, J., and Amiot, J.C. (1991). Ignition of Solid Propellants, *Rech. Aerosp.* 1991-2, pp.1-20.

113. Kubota, N., Ohlemiller, T.J., Caveny, L.H., and Summerfield, M. (1974). Site and Mode of Action of Platonizers in Double Base Propellants, *AIAA J.*, 12, pp. 1709-1714.

114. Steinz, J.A., Stang, P.L., and Summerfield, M. (1968). *The Burning Mechanism of Ammonium Perchlorate Based Composite Propellants*, AIAA Paper 68-658.

115. Niioka, T., Takahashi, M. and Izumikawa, M. (1979). Ignition of Double Base Propellants in Hot Stagnation Point Flow, *Combustion and Flame*, 35, pp. 81- 87.

116. Inami, S.H., McCulley, L., and Wise, H. (1969). Ignition Response of Solid Propellants to Radiation and Conduction, *Combustion and Flame*, 13, 531-536.

117. Thompson, C.L. and Suh, N.P. (1970). The Interaction of Thermal Radiation and M2 Double Base Propellants, *Combust. Sci. Technology*, Vol 2, pp. 59-66.

118. Kumar, R.K., and Kuo, K.K. (1984). *Flame Spreading and Overall Ignition Transient*, in Progress in Astronautics and Aeronautics *Fundamentals of Solid Propellant Combustion*, Chapt 6, in Series Progress in Astronautics and Aeronautics: Vol 90, *Fundamentals of Solid Propellant Combustion*, Edt. K. Kuo and M. Summerfield, AIAA.

119. Perzt A., and Kuo, K., Caveny, L.H., and Summerfield, M. (1973). Starting Transient of Solid Propellant Rocket Motors with High Internal Gas Velocity, *AIAA J.*, 11.

120. Caveny, L.H., Kuo, K. and Shackerford, B.W. (1980). Thrust and Ignition Transients of the Space Shuttle Solid Rocket Motor, *J. Spacecraft and Rocket*, 17.

121. De Luca, L., Caveny L.H., and Summerfield, M. (1973). *A Comparative Study of Radiation Ignition Characteristics of Different Classes of Propellants*, AIAA Paper 73-176.

122. Kassoy, D.R. (1974). *Homogeneous Explosion, Ignition to Completion*, AIAA Paper 74-150.

123. Hermance, C.E. (1975). Implications Concerning General Ignition Processes From Analysis of Homogeneous Thermal Explosion, *Combust. Sci. Technology*, 10, pp. 261-266,

REPORT NO.	AR NO.	REPORT SECURITY CLASSIFICATION
DSTO-TR-0068	AR-008-937	Unclassified

TITLE

Laser ignition of explosives, pyrotechnics and propellants: A review

AUTHOR(S)
Leo de Yong, Tam Nguyen and
John Waschl

CORPORATE AUTHOR
DSTO Aeronautical and Maritime Research Laboratory
PO Box 4331
Melbourne Victoria 3001

REPORT DATE	TASK NO.	SPONSOR
May 1995	DST 92/294	DSTO

FILE NO.	REFERENCES	PAGES
510/207/0091	123	74

CLASSIFICATION/LIMITATION REVIEW DATE

CLASSIFICATION/RELEASE AUTHORITY
Chief, Weapons Systems Division

SECONDARY DISTRIBUTION

Approved for public release

ANNOUNCEMENT

Announcement of this report is unlimited

KEYWORDS

ABSTRACT

This review critically examines the current state of technology of laser ignition of explosives, pyrotechnics and propellants. It presents the approaches used for each energetic material, looks at the materials tested, the results obtained and the potential for future development of in-service laser initiated ordnance.

It has been concluded that the only possible approach to laser initiation of explosives in a fuze is via a laser driven flyer plate but that the current cost and size of prototypes are too great for incorporation in most practical systems.

Laser ignition of pyrotechnics in terms of pyrotechnic materials and igniter design has reached a significant degree of maturity and it is only a matter of time before laser actuated pyrotechnic igniters are qualified for in-service use.

For propellants, the principle application of laser ignition technology is in the assessment of the overall hazard potential of the material with respect to planned and accidental stimuli, and in the verification of ignition theories and the determination of global energetic and kinetic parameters. In general solid propellants are initiated by pyrotechnic igniters and the practical development of a direct laser initiation system for rocket or gun propellants is not considered a possibility in the short term.

Laser Ignition of Explosives, Pyrotechnics and Propellants: A Review

Leo de Yong, Tam Nguyen and John Waschl

(DSTO-TR-0068)

DISTRIBUTION LIST

Director, AMRL
Chief, Weapons Systems Division
Dr R.J. Spear
Mr Leo de Yong
Dr Tam Nguyen
Mr John Waschl
Library, AMRL Maribyrnong
Library, AMRL Fishermens Bend

Chief Defence Scientist (for CDS, FASSP, ASSCM) — 1 copy only
Head, Information Centre, Defence Intelligence Organisation
OIC Technical Reports Centre, Defence Central Library
Officer in Charge, Document Exchange Centre — 8 copies
Senior Defence Scientific Adviser
Air Force Scientific Adviser, Russell Offices
Army Scientific Adviser, Russell Offices
Scientific Adviser - Policy and Command
Director General Force Development (Land)
Senior Librarian, Main Library DSTOS
Librarian, DSD, Kingston ACT
Serials Section (M List), Deakin University Library, Deakin University, Geelong 3217
NAPOC QWG Engineer NBCD c/- DENGRS-A, HQ Engineer Centre, Liverpool Military Area, NSW 2174
ABCA, Russell Offices, Canberra ACT 2600 — 4 copies
Librarian, Australian Defence Force Academy
Head of Staff, British Defence Research and Supply Staff (Australia)
NASA Senior Scientific Representative in Australia
INSPEC: Acquisitions Section Institution of Electrical Engineers
Head Librarian, Australian Nuclear Science and Technology Organisation
Senior Librarian, Hargrave Library, Monash University
Library - Exchange Desk, National Institute of Standards and Technology, US
Acquisition Unit (DSC-EO/GO), British Library, Boston Spa, Wetherby, Yorkshire LS23 7BQ, England
Library, Chemical Abstracts Reference Service
Engineering Societies Library, US
Documents Librarian, The Center for Research Libraries, US
Navy Scientific Adviser - data sheet only
ASTASS, CP3-4-12, Canberra ACT - data sheet only
SO (Science), HQ 1 Division, Milpo, Enoggera, Qld 4057 - data sheet only
Librarian - AMRL Sydney - data sheet only
Counsellor, Defence Science, Embassy of Australia - data sheet only
Counsellor, Defence Science, Australian High Commission - data sheet only
Scientific Adviser to DSTC Malaysia, c/- Defence Adviser - data sheet only
Scientific Adviser to MRDC Thailand, c/- Defence Attache - data sheet only